Acta Metallurgica Sinica (English Letters) (2024) 37:213–241
https://doi.org/10.1007/s40195-023-01631-7

Surface Modification Aspects for Improving Biomedical Properties in Implants: A Review

J. Sharath Kumar[1] · Rakesh Kumar[1] · Rajeev Verma[1]

Received: 22 July 2023 / Revised: 25 September 2023 / Accepted: 27 September 2023 / Published online: 11 December 2023

Abstract
The primary focus during surgery is to ensure successful implantation by achieving long-term and stable fixation of implants. Orthopaedic surgery is now more focused on the development of novel biomaterials intended to improve implant performance. To obtain a better understanding of metal implants, this article investigated the causes of material failures in certain cases and analysed a few case studies. The interaction between the implant and bone tissue was a crucial aspect of successful implantation, and this study explored the factors influencing this interaction as well as ways to improve it. Several modern approaches used for modifying implant surfaces were systematically illustrated and briefly analysed. Thermal spray coatings were often favoured because of their wide range of coating materials, but other substantial surface modifications (such as friction stir processing and laser surface texturing) were also used for a selection of applications. Notably, implant surfaces with desirable features, such as biocompatibility, antibacterial properties, corrosion resistance, and wear resistance, were essential for optimising implant functionality. This systematic review's main aim is to provide exhaustive reference information and a broad overview to advance the production and design of orthopaedic implants.

Keywords Biomaterials · Surface treatments · Thermal spray coatings · Antibacterial · Biocompatibility · Corrosion resistance · Wear resistance

1 Introduction

Metals are preferred over polymers and polymer–ceramic composites for implant manufacturing due to their strength and endurance. Metallic implants serve various functions, including permanent fixtures such as knee joints, hip joints, and spinal joints, as well as temporary implants such as screws, fracture plates, and pins. Stainless steel (SS), titanium (Ti), and cobalt–chromium (Co–Cr) alloys are the best options for replacing hard tissues, including joint implants, dental implants, and fracture plates. Due to the significant loads, mechanical stresses, and daily wear encountered by weight-bearing joints, implants must have a durable surface that is also compatible with the human body's environment [1]. It is anticipated that these implants will provide extended safety without complications for extended periods. Despite significant advancements in implant materials and designs, factors such as corrosion, wear of metal, bacterial infections, and more can still lead to implant failures, potentially shortening patient lifespans and posing life-threatening risks.

Corrosion and wear of implants are significant issues associated with metals, particularly for Co–Cr and SS-based alloys. When metals corrode, they lose bone density and become prone to failure due to diminished fatigue strength, reduced wear resistance, and stress shielding effect. Corroded implants of Ti alloy release Al and V ions [2], SS 316L release Cr ions [3], and similarly, Co–Cr alloys release Co and Cr metals [4]. These released ions combine with bodily fluids, leading to adverse reactions in bone tissues and contributing to the development of conditions such as Alzheimer's disease, dermatitis, and ulcers, among others. In some cases, these reactions have fatal consequences and therefore require additional surgery to remove the implant. For example, the corrosion and wear of Ti-6Al-4V alloy implants resulted in the release of Al and V ions, which dissolve into the host tissue and cause cytotoxicity [5]. Most

Available online at http://link.springer.com/journal/40195.

✉ Rajeev Verma
vermar@nitj.ac.in

[1] Industrial and Production Department, Dr B R Ambedkar National Institute of Technology Jalandhar, Jalandhar, Punjab 144008, India

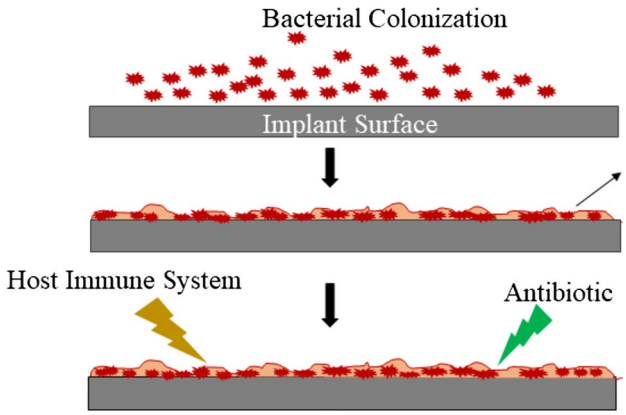

Fig. 1 Mechanism of biofilm formation on the implant surface

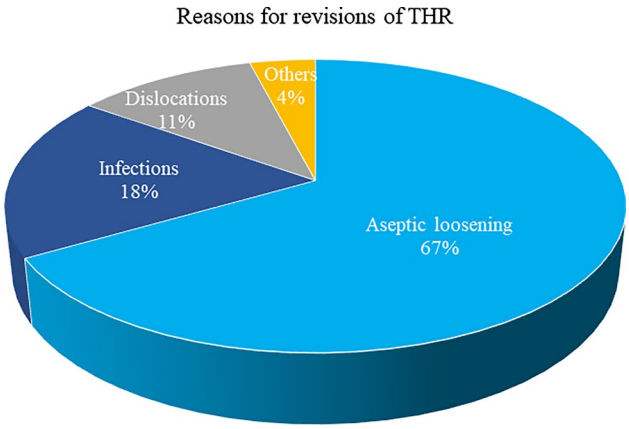

Fig. 2 Hip replacement implant failure reasons by percentage [10]

SS implants have reportedly failed due to pitting corrosion, resulting in pits, fractures, and bending in the implant, followed by tissue abrasion and discolouration [6].

Zhang et al. [7] identified bacterial infection and aseptic loosening as two significant challenges to control implant failures. Initial bacterial invasion on the surface of an implant leads to the formation of a biofilm on the surface, as shown in Fig. 1. This biofilm acts like a wall between the bacteria and the body's immune system, protecting them from antibiotics of the human body. Bacterial infections in the nearby bone and soft tissues prolong and worsen due to a proliferation of bacteria on the implant's surface. Aseptic loosening may result from poor initial attachment, mechanical loss, or induced bone loss around the implant. Any of these variables can cause early fixation loss and lead to aseptic loosening. Deterioration of implant contact, wear, corrosion, or small microorganisms can cause metal particle development on bone tissue [8].

The demand for implants has increased significantly as a result of the increasing number of arthritis patients and the evolution of lifestyles. According to a survey of 75.5 million people from 18 countries, it was projected that roughly 1.324 million primary and revision total hip and knee surgeries would be performed yearly, with an average rate of 149 surgeries per 100,000 people [9]. The causes of revisions of hip implants have been investigated by the Indian Society of Hip and Knee Surgeons (ISHKS), that data are presented in Fig. 2 [10]. Employing effective design and production strategies for implants that account for these factors is crucial. Metal implant problems can be effectively managed with the use of surface modification procedures [11].

Coating implant materials with biocompatible materials is an effective method to hinder metal wear. An appropriate selection of biocompatible materials for coating implants can reduce the negative body reaction while preserving implanted material functioning and durability. This is achieved by establishing a hydrophilic interface between the implant surface and biological fluids, thereby reducing adverse tissue reactions caused by implantation [12].

A concise overview of the significance of surface modification techniques applied to implants has been made by Liu et al. [11]. Liao et al. [13] published a review of extensively analysed cold-spray coatings applications in the biomedical industry, categorising them based on their specific functionalities. Ratha et al. [14] conducted a review study on hydroxyapatite (HA) coating on implants using plasma spray and analysed the effect of coating on improving surface properties. Junker et al. [15] studied the surface coatings and reported effect of coating on bone integration. Noticeably, no review article has been found that extensively reviews surface interactions, modification methods, surface properties, and their interrelationships. Undoubtedly, understanding the interplay among these three would lead to improvement of implant design. The focus of this review is to shed light on the research progression of surface interactions, modification methods, surface properties, and their interrelationships that may offer valuable insights for the development of robust and durable implants suitable for biological conditions.

The primary focus of this review is on metals and their alloys found in total hip replacement (THR) and total knee replacement (TKR). Given the vital role that hip and knee joints play in enabling mobility, these are subjected to tremendous loads and pressures. The next section of this study examines the materials used for these implants and potential post-surgery complications. The third section looks into the impact of surface interactions on cell and tissue growth, thoroughly examining aspects such as surface roughness, wettability, and porosity. Section four analyses biomaterial corrosion and its consequences for human health. Section five illustrates surface modification methods that lead to optimal properties, while Section six proposes properties of implant surfaces required, which can potentially improve implant functionality.

2 Materials Preferred for Implants

The selection of implant metals in the medical field depends on the purpose for which it is going to be treated. For these metals to be successful over the long term, these must be biocompatible and should possess certain properties. When an implanted material fails to achieve acceptable performance standards after surgery, it becomes a major issue since it can affect the expected recovery time and may necessitate additional surgical procedures. Therefore, it is crucial to emphasise the evaluation of the implant's biocompatibility as well as its mechanical, chemical, and tribological properties while paying special attention to the interaction of the material with the host environment [16]. Researchers must conduct several experiments while choosing the best materials for implants, as shown in Fig. 3.

Implants are now made from a wide range of metals and metal alloys, depending on the specifications of the individual. These implants can be divided into two groups: biodegradable metals like zinc [17], iron [18], and Mg alloys [19] and non-biodegradable metals like Ti alloys [5], Co–Cr alloys [20], SS [21], and Zr alloys [22]. Biodegradable metals gradually decay within the human body without posing any harmful risks. These are made in a special way to preserve their mechanical strength for a specific amount of time. The fact is that these biodegradable metals are less durable than their non-biodegradable metals.

Strength and adaptability to chemical environments are essential for hip and knee joint implants. As a result, titanium alloys, cobalt–chromium alloys, stainless steel, and zirconium alloys are favoured materials for these types of joint implants. The properties, advantages, and drawbacks of these metals are thoroughly discussed in Table 1.

Corrosion, wear, poor bone integration resulting in fibrous encapsulation, low fracture toughness, stress shielding, and bacterial infection are just a few of the causes of implant failure. Table 2 details particular case studies addressing these conceivable reasons for implant failure.

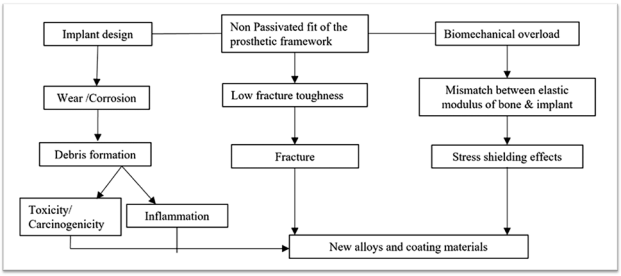

Fig. 3 The selection and acceptance of new material for implant [16]

2.1 Stainless Steel

Stainless steel (SS) was the first biomaterial cast for orthopaedic implants, due to its superior corrosion resistance which can be obtained through compositional modification by using addition of elements. SS is a ferrous alloy composed of Cr, Ni, Mo, Mn, Si, Cu, and C. Cr concentration greater than 12% enables the synthesis of chromium oxide (Cr_2O_3), this oxide which helps in stopping further oxidation and improves corrosion resistance [22]. 316L is the most prevalent grade of SS, because of its low carbon content it shows more persistent corrosion. However, when these were treated in an acidic environment for a long time, got failed due to corrosion [6]. In a study, fatigue corrosion was formed on an SS 316L implant, aided by crevice corrosion as shown in Fig. 4 [3]. Sulphur content in the alloy increased crevice corrosion and created crevice pits on the surface, which led to the failure of the implant.

SS 316L elastic modulus (200 GPa) is larger than human bone (10–30 GPa), causing excessive stress shielding at the tissue/implant interface and leading to SS 316L failure. Some studies reported Fe, Cr, and Ni which were released from SS 316L, reacted with surrounding tissue and led to swelling and decolourization of tissue [21]. Stainless steel is hugely used in temporary orthopaedic implants (fracture plates, hip screws) due to its low cost.

2.2 Titanium and Titanium Alloys

Titanium in its purest form has a low specific gravity, good corrosion resistance, particularly in salty solution (due to the formation of an adhesive covering of TiO_2), and can become deeply integrated with bone. So, Ti and Ti alloys have been successfully employed in the repair of bone fractures resulting from trauma, serving as a suitable alternative to SS. It is worth noting that Ti is a lightweight that can be further strengthened through alloying, as illustrated in Table 1. However, in cases of low mineral density bone, achieving the desired quality and union time of the reconstructed bone may prove challenging in implants [23]. Nevertheless, implants crafted from Ti alloys can offer strong bone–implant fixation under the physiological stress conditions experienced within the human body, thereby facilitating a high rate of fracture union [5].

The growing interest in using Ti alloys for tissue engineering has sparked the development of cutting-edge biomaterials. Commercial pure Ti (CP-Ti), Ti grade 4 (ASTM F67), and Ti6Al4V are the highly preferred alloys. Based on contaminants in Ti differentiated with grades, leading to some mechanical differences. Ti of commercial purity is

Table 1 Comparison of traditional implant material and their properties

Implant material	Typical applications	Advantages	Disadvantages	Mechanical properties		
				Young modulus (GPa)	Tensile strength (MPa)	Hardness (HV)
Natural bone [127]	–	–	–	3–20	130–180	40
Co–Cr alloys [20]	Prostheses stems, load-bearing components in total joint replacement	High wear resistance Corrosion resistance Easily castable	Hypersensitivity and inflammatory reactions are caused due to wear debris Higher modulus elasticity leads to bone resorption	210–240	655–1836	450
SS [21]	Fracture plates, screws, hip nails	High wear resistance Corrosion resistance Fatigue resistant	High friction coefficient, wear debris generation, aseptic loosening	190–205	586–1351	190
Ti and Ti alloys [5]	Hip and knee replacement prostheses, screws, and pins for bone fixation	Biocompatible Low stiffness Corrosion resistance	Poor tribological properties, low abrasive resistance, low mechanical stability, allergic reactions	105–114	760	340
Zirconium alloys [128]	Replacement of hip, knee, teeth tendons, ligaments, and bone filers	Biocompatible, Higher hardness	Bone resorption, higher wear rate, higher corrosion	150–199	200–495	1000–3000
Mg alloys [40]	Stents, Fracture plates, Screws	Biodegradable Mechanical properties equal to cortical bone	High corrosion rate, formation of H_2 gas, and premature loss of mechanical integrity	41–45	200	–
Iron [18]	Fracture plates, screws, thin-walled stents	Biodegradable Good strength and formability No gas generation	Corrosion rate is too slow, and	210	370	–
Zn alloys [43]	Fracture plates, Screws	Biodegradable Low reactivity in molten state Corrosion rate less than Mg	Poor mechanical properties, age hardening	75	90	–
UHMWPE [129]	Joint arthroplasty	Biocompatible, Abrasion resistance	Submicron particles of wear debris may contribute to osteolysis and aseptic loosening of the bone	0.9–2.7	53	62–66

Table 2 Case study reports of failed implants after surgery

References	Material	Implant	Survival time	Type of failure
Shahemi et al. [130]	UHWMPE	Acetabular cup of hip replacement	–	Failed due to aseptic loosening from wear generation 10 mm thickness of the cup was reduced to 2.3 mm (min) and 8.8 mm (max)
Affatato et al. [131]	Zirconium	Femoral head of joint replacement	The mean life of implants 6 years	In the study, most femoral heads failed due to aseptic loosening
Gervais et al. [132]	SS 316L	Bone-locking compression plates	–	High fatigue cycle, various stress risers in plate design, poor bone condition
Paliwal et al. [133]	Ti–6Al–4V & Co–Cr–Mo	Femoral hip prosthesis	Case i. 38 months Case ii. 28 months Case iii. 18 months	Two of the three failed catastrophically at the stem junction All implants failed due to fretting, pitting, plastic deformation, and stress-induced corrosion cracks There was evidence of metal ions released due to corrosion
Magnissalis et al. [134]	Ti6Al4V (porous coated)	Femoral stems	24 months	Microcracks formed on the surface due to high stress Due to porous coating, 75% of fatigue strength is reduced compared to uncoated
Shahgaldi et al. [135]	SS 316L	Femoral Nail plate	2.5 years	Wear, fatigue, stress corrosion

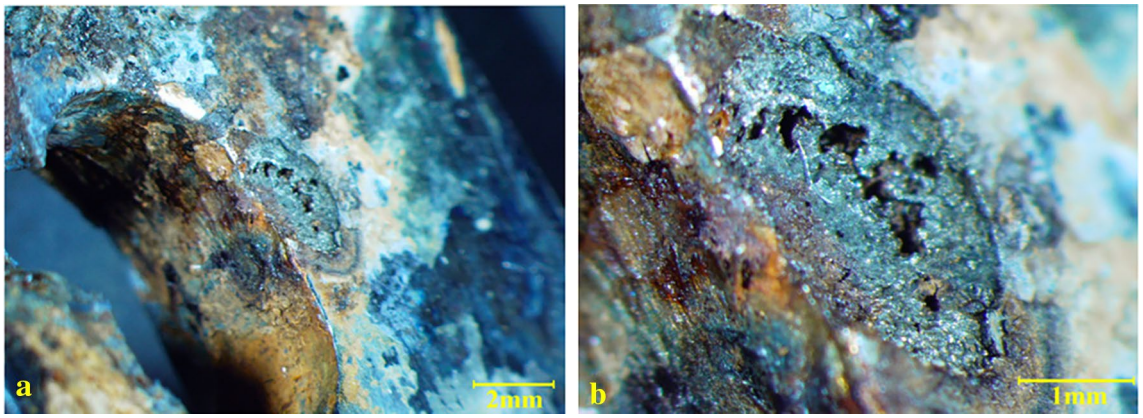

Fig. 4 Corrosive pitting areas of SS implant after two years of surgery [3]

graded according to its oxygen concentration. With increase in oxygen content, tensile and yield strength increases [24]. Due to vanadium (V) toxicity, different elements were utilised for alloying, including niobium (Nb), zirconium (Zr), and tantalum (Ta), these alloys exhibited good qualities; nevertheless, these alloys are still being studied [25, 26]. Ti's primary drawbacks are its comparatively expensive, less hardness, higher wear rate, and less bending strength. Cui et al. [27] 3D-printed Ti-35Nb-2Ta-3Zr using laser powder bed fusion which improved mechanical properties, exhibited higher compressive stress and strain with low modulus (4.7 GPa).

Released Ti ions from implant flow throughout the body, leading to harmful reactions such as yellow nail syndrome. Another possible cause of implant failure and adverse reactions is hypersensitivity responses. These metal ions can change the shape of proteins and even cause an immune response, which can cause damage to the organ. When released ions build up in an organ, these ions can change the work of metabolism and cause damage to the kidneys and heart [7]. In a study, through plasma spray, HA–TiO_2 was coated on a hip implant to improve corrosion resistance and biological performance as shown in Fig. 5 [28]. The uncoated samples have an inert TiO_2 layer with low adhesion strength, which prevented current flow in the corrosive medium and allowed current to flow in the medium, whereas the current density was reduced in the coated samples. Corrosion currents (I_{corr}) were determined to be 6.5 A/cm^2 for uncoated samples and 7.35 A/cm^2 for coated samples. The Mg 63 cells grew well on

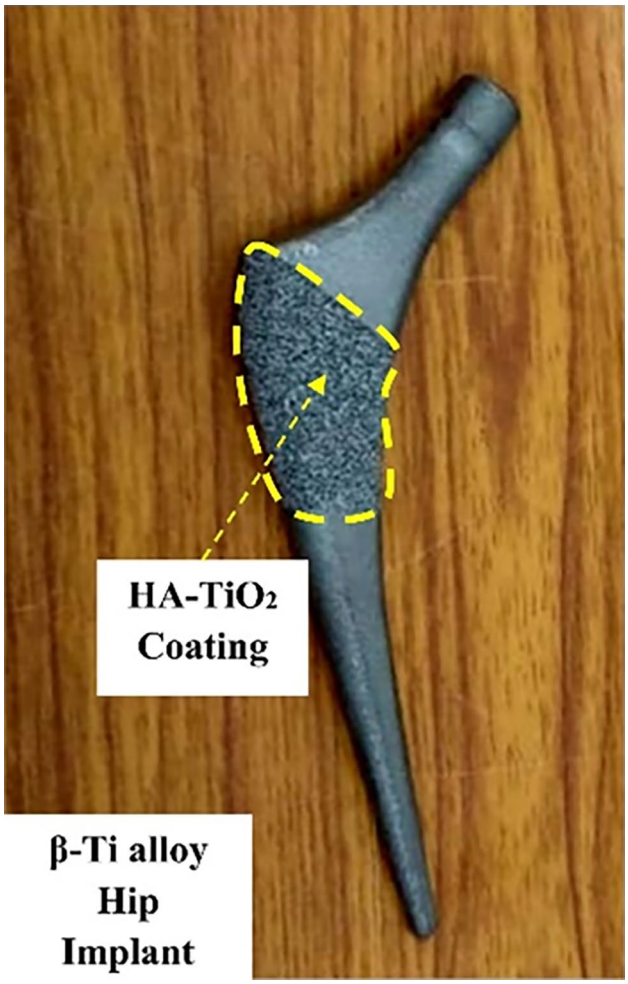

Fig. 5 β-Ti alloy hip implant coated with HA–TiO_2 [28]

the HA–TiO_2-coated substrate and proliferation was most significant on the coated surface.

2.3 Cobalt–Chromium Alloys

Cobalt (Co)–chromium (Cr) alloy is composed of 30–60% Co, 20–30% Cr, and a trace of other elements (Mo, Si, Ni, C). Because of their remarkable mechanical, biocompatibility, and corrosion resistance, as well as their potential survivability in hostile chemical environments, these alloys gained prominence in the early 2000s. Co-Cr alloys are preferred for a femoral head in hip and knee joints and as the ball component of shoulder replacements due to their corrosion resistance [29]. Co–Cr alloys have a lower osteointegration rate than Ti alloys. Because of their low integration with bone tissue, Co–Cr screws are easily removed once the fracture has healed. These have more strength than SS and Ti implants so, these are used to treat idiopathic scoliosis (spinal deformity) [30]. However, worries have been expressed about the potentially harmful chemical properties of the corrosion products produced by the deterioration of Co–Cr alloys in human body conditions. The released ions (Co^{2+}, Cr^{3+}, and Cr^{6+}) cause cell apoptosis, hypersensitivity, allergic dermatitis, necrosis, and genotoxicity [31]. To make Co–Cr alloys tougher and more resistant to wear, a great deal of research is going on. Singh et al. in 2019 to enhance Co–Cr alloy implant performance, Nb–Ta was coated using plasma spray [32]. This coating improved microhardness (400–700 HV); furthermore, an increase in Ta content was shown to further enhance microhardness. No microscopic fractures appeared on the coating's surface, enhancing its hydrophobicity. Enhanced biocompatibility and hemocompatibility have been attributed to the coating's resistance to corrosion.

2.4 Zirconium Alloys

Zirconium is more often used in dental implants because it works well with the body and looks aesthetically pleasing in tooth restorations. It was considered superior to Ti implants due to its lower risk of plaque accumulation, integration with soft tissue, and cosmetic appeal [33]. Zr implants had less bone resorption due to less Young's modulus, and stress carried on bone was less. Recently, Zr alloys have gained a lot of attention as a substitute implant material firstly, due to their in vivo experiments which showed intrinsic bone-like apatite layer on their surfaces, and secondly, intrinsically low magnetic susceptibility compared to all implant metals, including Ti, which offers better magnetic resonance imaging (MRI). Zr has better properties required for the implant material. However, the main drawback of Zr implants was wear and corrosion resistance, under excessive loading huge amount of implant material was removed in the form of wear. To improve its mechanical properties, Zr is often alloyed with Ti alloys.

Li et al. [34] in their study showed biocompatibility of Zr, Ta, and Sn in powder and bulk form, while bulk Nb and Ti were shown to be biocompatible, and their powder forms showed traces of cytotoxicity. Due to the less electrical conductivity of Zr, it has more adhesion resistance, which helps in a material's antibacterial properties. A study conducted by Scarano et al. reported that Zr oxides have more bacterial adhesion resistance properties than pure Ti and TiO_2 [35]. In a study addition of 5% Pd and Au reinforcement to Zr improved corrosion resistance [36].

2.5 Ultra-high Molecular Weight Polyethene

Ultra-high molecular weight polyethene (UHMWPE) is a homopolymer comprised of monomeric units of ethylene that are extensively cross-linked. The structure also yields polymers with molecular weights ranging from 3.5×10^6 to 6×10^6 kg/kmol, which can take the shape of fibres, plates,

or tubular structures depending on the type of medical grade UHMWPE. It is a vastly oriented thermoplastic fibre with an extremely crystalline structure (showing crystallinity greater than 90%), as well as biocompatibility, chemical inertness, high ultimate tensile strength (43.2 MPa), low wear volume (0.68 mm^3), low coefficient of friction, and low wear rate (0.15–0.2 mm/year), all of which contribute to its numerous biomedical applications [37]. UHMWPE is a polymer with significant clinical experience as a useful biomaterial for joint arthroplasties. Compared to other joint arthroplasties, THR and TKR have experienced a surge in the utilisation of UHMWPE bearing components of hip implant as acetabular cups. A study has shown that using UHMWPE as a linear material between metal–metal femoral heads causes a lot of wear, and this debris causes inflammation, which leads to osteolysis and loosening of the implant [38]. Birman et al. (2005) conducted a case study on 120 patients in which 113 acetabular cups were retrieved, primal reasons for failure followed by aseptic loosening (22%), infection (16%), dislocation (25%), wear (20%), pain (4%), and osteolysis (8%) [39]. The cup failure is shown in the form of cracks, impingement and oxidation as shown in Fig. 6.

2.6 Magnesium Alloys

Magnesium alloys are modern biodegradable metals with good osseointegration properties. Mg alloys are lightweight materials, their density (1.74–2 g/cm^3) is closer to cortical bone (1.8–2.1 g/cm^3), and mechanical properties of these alloys are almost equal to human bone [40]. So, there will be less stress shielding effect on the implant. One disadvantage of Mg alloys is low corrosion resistance, it gets corroded in months [41]. Released Mg reacts with water and releases hydrogen gas, this emitted gas can enter the bloodstream and cause severe medical complications. Furthermore, the creation of hydrogen gas bubbles may impair osteocyte connection, leading to callus development and

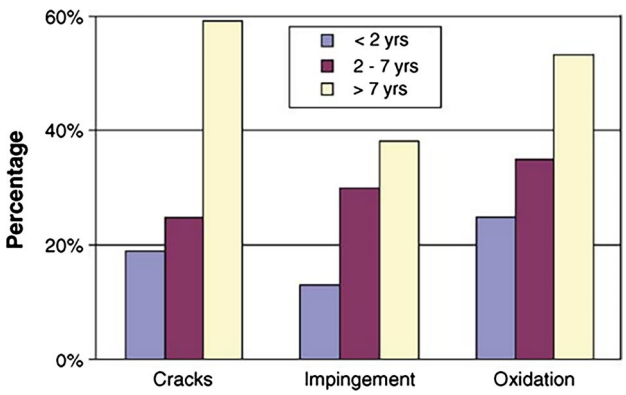

Fig. 6 Gantt chart of UHMWPE acetabular cup failures due to various reasons with time duration [39]

cortical abnormalities. The emission of H_2 is reduced to 0.01 ml/cm^2/day when Mg is alloyed with Zn, Al, and Mn components [19].

2.7 Iron

Iron is a potent metal as a biodegradable implant because of its exceptional mechanical properties. Due to high elasticity and high radial resistance, iron is ideally suited for the fabrication of thin-walled implants. In addition, iron possesses a high degree of ductility, which is advantageous in the implantation process, where the material endures plastic deformation [18].

The journey of biodegradable metals began with the invention of the iron stent made from Armco iron (Fe > 99.8%). This was transplanted into the descending aorta of white rabbits in 2001 in New Zealand [18]. There were no substantial signs of inflammatory response or systemic toxicity in the surgical outcomes. However, the biodegradation rate of 0.16 mm/year and the inherent ferromagnetic properties of pure iron prevented its use as implanted material [42]. To address these issues, a minor amount of manganese was incorporated, resulting in a 0.44 mm/year acceleration in degradation rate. Nevertheless, this rate is insufficient for extensive applications.

2.8 Zinc Alloys

Zinc-based alloys show promise as potential biodegradable implant materials. Due to their low melting point and reactivity, molten zinc-based metal alloys can be easily fabricated by melting, gravity casting, air die casting, or heated forming [43]. According to studies, zinc alloys do not manifest local or systemic toxicity or other biological compatibility issues. Degradation and biocompatibility of zinc satisfy the criteria for biodegradable material. However, the limited mechanical strength of pure zinc as a biodegradable implant material is a noteworthy disadvantage [17]. The ultimate tensile strength (UTS) of Zn in cast and wrought conditions is only 20 and 120 MPa, respectively.

2.9 High Entropy Alloys

High-entropy alloys (HEAs) are drawing attention as a potential metal alloy. To develop a stable solid solution alloy, the concept of HEA arose to develop a single-phase solid to improve the mixing entropy of the material. These alloys contain a large number of distinct elements; hence these are also called multi-principal element alloys (MPEAs) or complicated alloys. HEAs may contain single or two-phase structures, regardless complexity of the composition [44]. HEAs comprise at least five elements for which all lattice sites have the same probability of occurrence. The disparity

in atomic radius creates a lattice distortion in the crystal structure as the solid solution is created. When the lattice distortion energy is excessive, crystals lose their capacity to maintain their structure and create amorphous phases or intermetallic compounds. Whether the material is amorphous or crystalline, this distortion will impair its functional properties [45].

HEAs in a biomedical sector still in the early stages, according to the present literature HEAs preferred in medical implants are refractory metals that are safe for patients with allergies. Ti, group IV, and group V elements, with Cu and Co elements, make up the bulk of biomedical HEAs [46, 47]. Gurel et al. [48] described the mechanical properties and failure mechanisms of the TiTaHfNb, TiTaHfNbZr, and TiTaHfMoZr systems, which were evaluated for strength using impact loading. Zr and Nb increased corrosion resistance in the three HEAs, after experimentation in simulated body fluids (SBF) and AS (artificial saliva) solutions, scanning electron microscopy (SEM micrographs showed no substantial corrosion on TiTaHfNbZr but, TiTaHfNb showed corrosion in SBF medium [49]. After 28 days of immersion, the alloy with Mo released more ions than the alloys with Nb and Zr, which were stable. When Zr and Mo were added, the dislocation activity in the microstructure was changed under impact stress. TiTaHfNb and TiTaHf alloy systems were, respectively, weakened by these two elements, rendering them less resistant to impact and more brittle.

HEAs with a biomedical application potential are treated as Bio-HEAs. Feng et al. [50] devoted considerable time to reviewing Bio-HEAs, and discussed the mechanical, physical, chemical, and biological properties of Bio-HEAs in the study. Bio-HEAs have tremendous potential as implants; these showed enhanced corrosion resistance, wear resistance, and biocompatibility; however, these results were obtained in the laboratory and not in clinical trials. Bio-HEAs are not yet extensively used due to their intricate preparation process, high production and material cost, and lack of clinical testing.

In general, biomedical protective coatings must possess several desirable properties, such as a low modulus of elasticity, stability in chemical, corrosion and wear resistance in SBF, a low coefficient of friction, biocompatibility, and good adhesion of cells to the surface on which these are coated. HEAs can be produced by mixing different elements to attain certain desired properties. While HEAs have the potential to be good coating materials for biological applications, they must first meet certain HEA criteria.

Currently, numerous metals and non-metals are utilised for orthopaedic implants based on their specific properties and intended functions. However, post-operative complications pose a major problem for surgeons and their patients. As a result, scientists are actively looking at various biomaterials as viable remedies to deal with these issues. In addition, researchers are investigating the potential for surface modifications to improve both these implants' effectiveness and durability.

3 Influencing Factors of the Interaction Between Bone Cells and Implants

For the creation of an efficient surface for orthopaedic implants, it is essential to comprehend the interaction between osteogenic (bone) cells and surfaces with micro- and nanoscale features. Numerous studies have been performed to understand the effect of surface features on the adherence of osteogenic cells. The following section looks at how surface roughness, microtopography, nanotopography, porosity, and surface energy affect osteogenic cell behaviour.

3.1 Micro-topography

Microtopography of implants refers to the surface features and textures at a very small scale on the surface of medical implants, particularly orthopaedic or dental implants. Microtopography is essential for enhancing the implant's ability to osseointegrate (bond with bone tissue) and enhancing its long-term stability and functionality. Bone-to-implant interfaces are created when osteogenic cells unite and deposit bone into the surface's imperfections. Roughened surfaces modified with certain acids may enhance bone bonding and bone formation. Sandblasted and acid-etched surfaces were used to improve bone adhesion in histomorphometry analyses [51].

A study shows that the roughness of the femoral head and acetabulum affects wear in a way that both surfaces (UHMWPE and TiN-coated SS) are dependent [52]. A pin-on-disc test showed that a UHMWPE part with a smooth roughness (0.022 µm) had less wear with a smooth counter-face (wear 0.01 µm) and with a rough counter-face (wear 0.04 µm). When both surfaces were rough, this was the worst-case scenario, but making both surfaces less rough is not a good solution. Polishing the hard TiN counter-face got the least amount of wear. On the other hand, Jahani et al. [53] studied that increasing surface roughness was not helpful all the time, it increased abrasion which eventually ended in poor bone metal bonding. In this observed that the formation of cracks was quick if surface roughness was above 40 µm.

A study found that a bone–implant's interfacial shear strength may be greatly improved by creating a rough surface with optimum microgeometry [54]. An optimal surface would include several, closely spaced pits, each with a diameter greater than some threshold, a depth sufficient to not limit shear strength along fracture planes. According to ISO 7206-2:2011, femoral heads should meet the specified criteria, with the maximum allowable values for average

roughness (R_a max) and total roughness (R_t max) being 0.05 and 1 µm, respectively [55]. Ren et al. [56] studied the effect of surface on cell adherence by creating four different surface polished surfaces (P), additive manufacturing (AM), additive manufacturing with post-treatment of electron beam machining and acid etching (AE), and another sample with anodic oxidation (AN). Figure 7 shows the surface of cells in groups P, AE, and AN had a big spreading area and a stretched polygonal shape filled with pseudopodia. Nonetheless, cells belonging to the AN group had a longer lamellipodia extension length and more filopodia on the border. These pseudopodia are critical structures for cell adhesion and migration on the material surface. The cells in group AM, on the other hand, had a thin spindle shape with a small area where they spread out. This showed that the original surface shape of the 3D-printed Ti-6Al-4V sheet was not helping the cells stick to it. According to this study, there are four steps of cell growth: proliferation, differentiation, mineralization, and apoptosis. Samples of AE and AN have positive effects on cell differentiation and mineralization phase; after 21 days of observation, cell proliferation rates were measured.

3.2 Porosity

Porosity in implants implies the existence of tiny, interconnected voids or pores within the implant's substance. During the manufacturing process, these pores can differ in size, shape, and distribution and are purposefully designed or controlled. Surface porosity improves osteointegration by letting osteogenic cells grow into the implant, which strengthens the implant and bone interaction. Porous implants are much lighter than their dense counterparts and allow cells to grow and new bone to form. Numerous researchers have investigated the effect of pore size and morphology on osteoblast differentiation and integration. The majority of researchers have concluded that scaffolds with interconnected pores promote superior bone growth than those with closed pores. This is because the blood vessels grow better, making it easier for osteoprogenitors (bone stem cells) to reach the bulk of the scaffold. Also, it has been said that the pores must be big enough for vascular infiltration without affecting the mechanical properties of the implants [57]. Yet, holes bigger than 1 mm are not good for implants to last longer, which tends to grow fibrotic tissue inside of bone. Studies in this area agree that the best pore size is between 100 and 700 µm, based on the shape of the pores and the materials used to make the scaffolds [58]. Singh et al. [59] 3D printed SS 316 l fracture plates with 34% porosity.

Yan et al. [60] finite element approach was used to model the stress and strain field of the femur following hip arthroplasty to investigate how a porous Ti femoral prosthesis affected bone repair by analysing bone density loss. The study examined Co–Cr alloy, Ti alloy, and porous Ti with various porosities to analyse bone reconstruction. Observed that using porous Ti in place of Co–Cr implants would significantly reduce bone volume and density. In a study, increasing porosity (20–60%) showed bone density decreasing linearly with increase in porosity, but porous Ti became weaker in strength shown in Fig. 8. According to the study, porous Ti reduces stress shielding around the implant after THR [61].

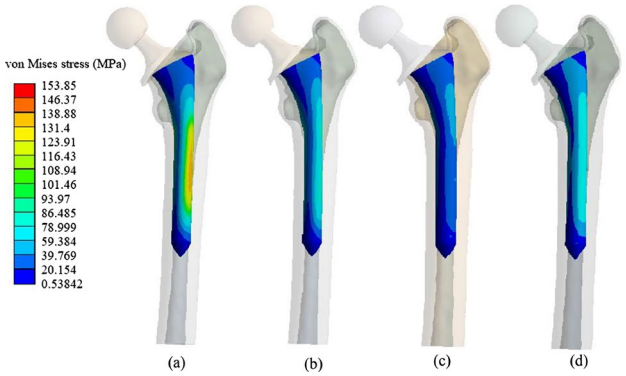

Fig. 8 Hip implant femoral stems stress distributions: **a** without any porous (fully dense), **b** femoral stem with 40% porous structure, **c** femoral stem with axial graded porous structure increased distally, **d** femoral stem with radial graded porous structure increased inwardly [61]

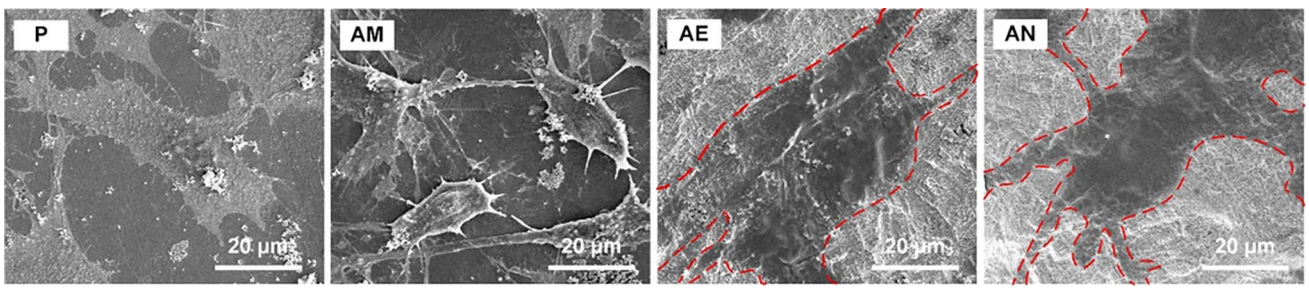

Fig. 7 SEM images of MC3T3s cell morphologies after 48 h of adhesion [56]

3.3 Surface Energy

Surface energy is important in defining how implants interact with biological tissues, cells, and fluids, and it can influence the effectiveness of the implantation procedure as well as the implant's long-term performance. The bonding potential of a substance determines how many interactions it may participate in with fluid; therefore, hydrophilic materials have high bonding potentials. Higher wettability leads to a better distribution of mineral phases, which speeds up the response of cells at the interface between the implant and the tissue and speeds up the rate of healing. But hydrophilic surfaces have molecules that are strongly bound to water molecules. This makes it hard for proteins to move water molecules, which makes it harder for platelets and fibrinogen proteins to stick to the surface. So, some authors think that hydrophilic surfaces are very wet and perhaps not considered the best option [62].

When a surface is hydrophobic, the attraction between the surface and water molecules is weaker. It is easier for proteins to replace water molecules, making it easier for platelets to stick to the surface [62]. The implant's free energy is a crucial determinant in protein adsorption. The free energy needed for biomedical implants typically falls in the range of 1–3 ($\times 10^{-6}$ kJ/m^2). Hydrophobic surfaces have a lower energy need for protein adsorption (< 1.3 kJ/mol) because proteins can easily replace water or any fluids and a higher energy requirement for hydrophilic surfaces (> 1.3 kJ/mol), hence these tend to adsorb more proteins [63].

To summarise the impelling factors and enhancing the interaction between tissue and implants can be realised by increasing the porosity of the surface within a diameter range of 100–700 µm. Although it was believed that the presence of microstructures on surfaces had a positive impact on cell differentiation than mirror polished surfaces, nanostructured surfaces did not show much impact on cell growth. However, excessive inhomogeneous surface roughness promotes bacterial growth and facilitates the formation of biofilms. Moreover, the introduction of surface roughness within a range less than 1 µm has been shown to facilitate cell and tissue growth within the grooves. Contrary to the initial belief, experimental studies have disproven the fundamental concept of favouring hydrophilic surfaces, indicating that hydrophobic surfaces are more beneficial.

4 Corrosion in Biocompatible Material

Corrosion of biomaterials is defined as the deterioration or degradation of metals in a chemical environment. When electrons transfer from anode (loss of metal ions) to cathode (gain of metal ions), corrosion occurs because of the lower chemical energy of material thermodynamic forces [64]. For

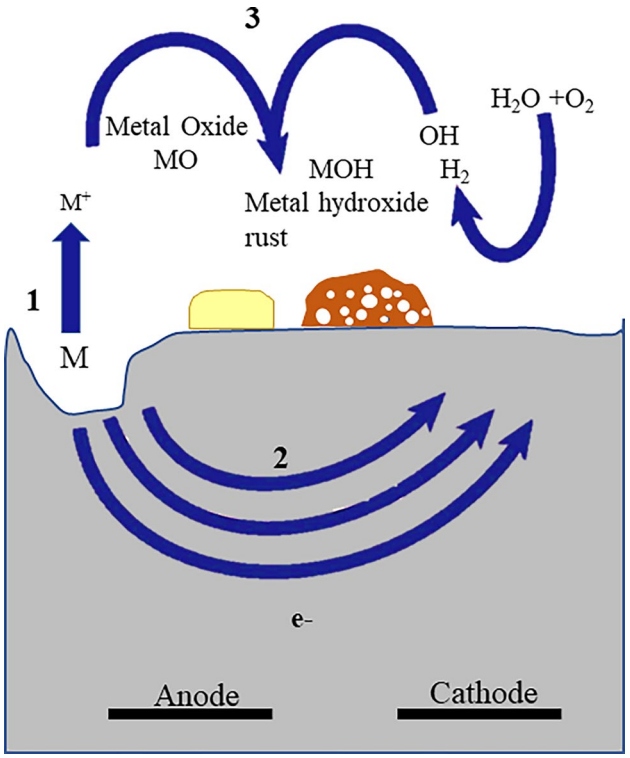

Fig. 9 Corrosion on a surface: (1) on the surface of an aqueous environment, the metal dissolves and cations are eliminated (oxidation); (2) remaining electrons are drawn to a differential charge at another surface location (reduction); and (3) metal-oxide or metal hydroxide form as by-products of this reaction [65]

this exothermic reaction, low activation energy is required to trigger the process. Metals exposed to air or aqueous solutions without a protective metal-oxide layer experience a severe exothermic reaction shown in Fig. 9 [65].

The majority of bodily fluids consist primarily of solutions containing sodium (Na^+), chloride (Cl^-), and 0.9% saline, along with various small ions. Under typical conditions, these fluids contain different types of amino acids and soluble proteins. In addition, they transport minute quantities of cellular debris, which play a vital role in the formation of essential interactions with implants. These solutions typically maintain a pH level between 7.2 and 7.4 at 37 °C and 1 atm, keeping them nearly neutral. However, in cases of irritation caused by injury or surgery, the pH of bodily fluids can drop as low as 3–4, primarily due to the release of inflammatory cells [66].

The human body can create a hostile environment for any implanted material, which is worsened by fluctuations in ionic strength, which are frequently caused by factors such as high blood pressure or the accumulation of specific ions. Furthermore, the partial pressure of oxygen inside the body is roughly one-quarter of the atmospheric pressure, which can accelerate the corrosion of implants by slowing down

the formation of protective films of oxide on the implants. The oxide coating that forms on metal surfaces is essential since it prevents metallic ions from escaping. The surface oxide's behaviour changes when metallic ions escape. In addition, composition of oxide coating on the surface is altered by the reaction of tissue with metal [67].

4.1 Types of Corrosion in Metal Implants

Corrosion of implants varied widely depending on implant metal, geometry, and environment. The most frequent types of corrosion seen in implants are crevice [68], pitting [69], and tribocorrosion [70]. Pitting corrosion is the result of a localised relative breakdown of the passive film, i.e., rupture of the passive film. This rupture reduces the energy required for the activation energy barrier for corrosion [65]. Pitting is a form of localised corrosion by the creation of cracks on metal surfaces. It typically arises on substrates, which were inherently protected by a thin oxide film. In the presence of Cl in the environment, the film degrades locally and cavities form due to the rapid dissolution of the underlying metal. In general, pitting corrosion can be approximately classified into three stages: (1) nucleation of pitting, (2) metastable pitting, and (3) propagation of pitting [71]. Metastable pitting corrosion is harmful to metallic biomedical materials because it frequently results in substantial ion release from the dissolved metal matrix, thereby reducing the implant's lifespan [2]. Crevice arises between adjacent surfaces or in confined spaces, like places where there is no possibility of oxygen exchange. The reduction of PH value and the rise of Cl ions are two critical factors in the instigation and spread of crevice corrosion. As the acidity of the surrounding environment rises over time, the passive layer of the alloy dissipates and the local corrosion process accelerates. This condition happens when the crevice environment becomes more corrosive than pitting corrosion. Additionally, localised corrosion may emerge as pitting. Tribocorrosion, which originates during wear and fretting and advances rapidly, can lead to metal failure even without corrosion formation.

Crevice corrosion is commonly observed in hidden regions, such as the interfaces between screws and surface or below sealing components. When implants are subjected to environments containing chloride, materials such as SS 316L and similar passive alloys typically exhibit crevice corrosion [3]. In the case of SS 316L, corrosion that forms in the spaces between the screw heads releases Cr ions, which could have contributed to the high blood levels of Cr. Carcinogens are released into the human body through pitting corrosion of Co–Cr alloys [72]. Although Ti and its alloys are resistant to pitting corrosion under a variety of in vivo conditions, these are vulnerable to corrosion in high-fluoride solutions [73].

4.2 Impact of Corrosion on Human Health

As the implant degrades within the body, it releases metallic ions that interact with diverse biological fluids. If the metal particles are not surgically removed, the surrounding tissues may become inflamed. Table 3 provides a summary of their corrosive effects on the human body. In corrosion process dissolved metals, transform into a fragile and easily breakable state. When cracks appear on the material, more surface area is exposed, removing the protective oxide layer and accelerating the corrosion rate [74]. Wear is the major cause of failure of orthopaedic implant, which accelerates corrosion over time. As a result, wear-resistant materials such as Co–Cr alloys and ceramics are widely used to manufacture implants. For hip implants, Ti and its alloys are only used to create the femoral component, while Co–Cr alloys or other durable ceramics are used to create the ball. Sometimes, the parts of the femoral are wrapped with cement to make sure they stay in place well. Researchers have found deteriorated particles in tissues around implants and organs including the kidney and liver. This suggests that the release of corrosion products can trigger unfavourable biological reactions in the host. The tolerable corrosion rate for metal implants is approximately 2.5×10^{-4} mm/year, which is equivalent to 0.01 mils/year [75].

Chen et al. [2] conducted experiments on Ti-6Al-4V and observed that the release of Ti and Al ions in dynamic Hank's solution (Ti-0.0011 and Al-0.0516 Mg/L) significantly more than stable (Ti-0.0363 and Al-0.0516 Mg/L). A wide variety of diseases, including Alzheimer's disease and osteoporosis, may be precipitated by excessive Al ions. Amel-Farzad et al. [3] conducted a case study to determine the causes of SS 316L implant failures; corrosion fatigue was the leading cause. A large debris of Cr and Ni ions was found in fracture tissue which was detected by energy disperse spectroscopy (EDS) analysis. CoCrMo alloy has remained a widely favoured material for artificial hip prostheses, because of its remarkable durability against wear and corrosion. Nevertheless, the release of ions like Co and Cr from these implants during in vivo degradation has resulted in several adverse consequences, as well as

Table 3 Effect on the human body due to increased metal ions

Biomaterials	Effect
Nickel [136]	Have an effect on skin (dermatitis)
Cobalt [137]	Anaemia B inhibits iron from being absorbed into the bloodstream
Aluminium [138]	Alzheimer's disease
Chromium [139]	Ulcers and damage to nervous system
Vanadium [140]	Toxic in the elementary state

osteolysis, soft tissue reactions, bone necrosis, and chromosome abnormalities [4].

In practical scenarios, metal implant degradation begins at initiates at the surface layer. The corrosion resistance, wear resistance, and biocompatibility of Ti and its alloys are significantly impacted by the properties of the surface layer. By creating protective or biocompatible layers on the exterior of Ti and its alloys, it becomes possible to enhance their longevity and reliability when exposed to biological conditions [76]. Some surface modifications on Ti and its alloys, improved cell adhesion and/or antibacterial properties [28, 77, 78]. Kedia et al. [79] used laser surface texturing (LST) on SS 316L to improve the corrosion resistance and this surface modification enhanced cell adhesion. The tribological properties of Co–Cr alloys were improved through laser treatment by Wei et al. [80]. In order to further enhance the efficacy of metals, over the past 50 years, a wide variety of surfacemodification methods have been implemented.

5 Surface Modification to Improve Corrosion Resistance

Surface modifications of implants are done with the aim of enhancing their biocompatibility, durability, and overall performance within the human body. These modifications can act as a protective layer to protect the implant from corrosion and wear. Engineers and scientists will remain committed to enhancing the surface properties of biomaterials as long as implants continue to encounter challenges associated with insufficient cell adhesion and the debris of wear and corrosion. There were many surface modification methods used, but only some of those are listed in Table 4. It is essential to note, however, that each of these approaches has inherent limitations. In the subsequent sections, examined some of the most prevalent surface modification approaches.

5.1 Grit Blasting

To improve osseointegration in weaker bone structures, increasing the surface roughness of implants with practical and economical approaches such as micro or nanoparticle blasting has become popular. Particulates, often sand, alumina, Al_2O_3, Al, Ti, or HA, are driven into the implant surface using a high-pressure and high-velocity sandblasting device [81]. As a result of the deformation of the base material, multiple depressions are formed, the size of which depends on the composition and size of the applied particulates. Attained, however, surface homogeneity is frequently jeopardised. This process removes rust, scales and other contaminates from the surface. In a study, grit blasted surface of Ti was found approximately five times the shear strength of a smooth surface [76].

5.2 Additive Manufacturing

These AM techniques, which build components layer by layer based on their computer-aided design (CAD) models, were first created in the 1980s [82]. AM technologies are unconstrained by the limits imposed by traditional manufacturing processes and may generate components with far more complicated forms [83]. AM covers the ability to biomimetic extracellular matrix (ECM) and the ability to create adaptive scaffolds for uniform cell dispersion regardless of the intricacy of the morphology. The most significant barrier is the scarcity of biomaterials with the essential stability and inherent qualities for printing scaffolds. Xu et al. successfully printed Ti6Al4V-6Cu alloy using selective laser melting (SLM) and investigated the properties and biological

Table 4 Categorised surface modification methods and their features [11]

Category	Techniques	Features	References
Physical methods	Shot Penning	Simple and low cost Promote attachment the both of tissue cells and bacteria	Jemat et al. [81]
	Additive manufacturing	Creating complex 3D structures Material saving	Yuan et al. [141]
	Thermal spraying	Economical and safe	Tang et al. [142]
	Laser treatment	Achieving complex and precise topography	Hindy et al. [143]
	Magnetron sputtering	Strong adhesive and homogeneous coating can produce	Liu et al. [85]
	Friction stir processing	Without melting metal, Uniformity in corrosion	Shunmugasamy et al. [101]
Chemical methods	Anodizing	An accelerated electrochemical process	Hall et al. [108]
	Sol–gel	Low-temperature technique Drugs delivery	Adams et al. [144]
	Alkali treatment	Extending uniformly Do not damage mechanical properties	Yao et al. [145]

responses of Cu-modified Ti6Al4V alloy [84]. It was discovered that adding Cu to Ti6Al4V alloy can effectively boost the rate of cation release without compromising the cell viability of gingival fibroblasts and osteoblasts. Moreover, by reducing macrophages, the Ti6Al4V-6Cu alloy promotes angiogenesis and lowers local inflammation. Because of the rapid heating/cooling cycle in SLM processing, Ti-6Al-4V alloy generated by SLM had distinct microstructures when compared to traditional counterparts [23].

5.3 Magnetron Sputtering

During the sputtering procedure, a strong ion beam was generated in a glow and discharged plasma was directed toward target (or cathode) plate. Target atoms may condense on a substrate following removal (or "sputtering") from the bombardment process. Magnetron sputtering involves adding a closed magnetic field to the sputtering target, which enhances electron travel time, lowers the number of scattered atoms, and enhances ionisation efficiency. Liu et al. (2021) conducted research for improving the wear resistance of porous Ti6Al4V substrate for artificial joint implants, using HEA ($Fe_{25}Co_{25}Ni_{25}Al_{10}Ti_{15}$) film coating with magnetron sputtering [85]. This study observed at pd 30 µm porous gap less wear of material removed and due to porous structure modulus difference between bone and tissue reduced which helped in eliminating stress shielding. Magnetron sputtering is widely used for the deposition of HEA in biomedical applications. But many drawbacks in this homogeneity of coating are not achieved effectively and lower surface roughness is not possible.

5.4 Thermal Spraying

Thermal spraying is a technique employed to create fibrous coatings by adhering a material to the surface of a substrate under high-pressure gas spraying conditions, typically when the material is molten or partially molten. This method can be used to improve the biocompatibility, durability, wear resistance, and overall performance of implants. Plasma spray (PS), high-velocity oxygen fuel spraying (HVOF), and cold gas dynamic spray (CGDS) are currently the most common thermal spray coating techniques.

5.4.1 Plasma Spraying

PS involves melting and propulsion of powder particles in a small compartment toward a surface with a high energy heat source. These droplets quickly begin cooling and solidifying upon interaction with the surface of the component, due to a heat transfer phenomenon between the component and the droplet. The particles in the plasma spray flow at a speed of 100–300 m/s (30 and 90% of the speed of sound), and a temperature of between 8000 and 14,000 K. The particle speed ranges around 20–90 m/s, with the size of feedstock [86]. There are various factors that affect the plasma spray process, and when it comes to biomaterials, particle coating phase structures are significantly impacted by the pressure of the plasma environment. Due to the high number of operating parameters and the intricate interactions that exist between them, optimising the plasma spraying process is a challenging and expensive endeavour.

Due to its fast deposition rate and low cost, the plasma spray technique is the most frequent method for depositing HA coating over the metallic implant [14]. The high temperature in the plasma process causes the breakdown of HA particles into amorphous calcium phosphates. A study found degradable amorphous phases are beneficial to improve bone integration [87]. In a study, HA-Nb plasma spray coating was performed on Mg alloys to slow down the corrosion [88]. The coating was done with varying proportions of Nb as 10, 20, and 30% with HA. In the X-ray diffraction (XRD) analysis, it was discovered that a gradual increase in Nb improved the crystalline HA phase. Amorphous calcium phosphate was shown in XRD, which appeared due to the breakdown of HA when it was exposed to high temperatures in the coating. Higher thermal conductivity of Nb led slower rate of cooling in HA zones, which led to more brittleness in coating. In another study, Ti implant surfaces are coated with a novel bi-layer HA/Al_2O_3–SiO_2 nanocomposite using a plasma spray technique [89]. The results confirmed that the roughness of the double-layered nanocomposite plasma-sprayed coating is enhanced in contrast to the single-layered structure of the HA coating, along with other qualities such as wettability, cell survival, and proliferation. PS composite ceramic coatings are preferred for enhancing wear and corrosion resistance properties [90]. These ceramic coatings also improved the interaction of tissue and bone through enhanced cell growth [91].

5.4.2 HVOF Spraying

In HVOF spraying, high-speed flame is produced with gas or liquid fuels (like propylene, propane, hydrogen, and kerosene) and O_2. In this method, the coating materials are pushed into the stream of hot flames and moved quickly toward the target substrate by an inlet. Melted or partly melted particles are driven onto the substrate at 1000 m/s depending on feedstock density, shape, and particle size. HVOF coatings are thick, well-bonded, and have fewer oxides because their particles move faster so, the less flight time for the particles to get oxide [92]. Also, the HVOF process coatings produce a smoother surface that has a high density and no interconnected pores. These coatings are harder, have less porosity, and have stronger bonds than flame spraying and plasma spraying so, these are preferred

for wear and corrosion-resistant applications. Biocompatible coatings benefit from HVOF.

In the past few years, nanostructured coatings have received a lot of attention because of their better mechanical properties. Nano-sized ceramics like aluminium oxide and Ti oxide could help osteoblasts stick to them better [93]. So, nano-sized particles in biocompatible coatings could have a good effect. HVOF spraying was used to coat nanostructured Ti + HA composite for biomedical applications, because of their mechanical performance, a stable nanostructured TiO_2 phase formation, and a bioactive HA phase that can improve the performance of the deposited coating [94]. Also, heat-treated samples of HA composite coating had shown good effects. Heat treated at 750 °C for 30 min made the coating more uniform of HVOF-sprayed HA/nano-Zr composite sample. One study found that as the speed of the flame stream goes up, the coating layer's porosity goes up due to the powder particles speed. But both the speed and the porosity can be controlled in real time [77]. Focus turned to HVOF-sprayed HA and HA/TiO_2 functionally graded coatings for producing long-lasting, durable biomedical coatings with improved mechanical resistance. This cutting-edge method enabled a direct comparison between the benefits of a multi-layered coating design and those of a conventional single-layer coating with real-world biological applications.

5.4.3 Cold Gas Dynamic Spraying (CGDS)

CGDS, a late 1980s spray technology, was developed because of inevitable issues arising in thermal sprayed coatings. It can deposit sensitive materials to oxygen or temperature, like nanostructured and amorphous powders. CGDS is environmental friendly, it works based on the kinetic energy of particles, and low-temperature rates make it better than other spray techniques. Low-temperature CGDS uses plastic deformation of the material for coating. Particles (5–50 µm) are amplified by a preheated gas temperature (250–1100 °C) which is lower than the material melting point and sent at supersonic speeds (300–1200 m/s) toward a prepared substrate. As the gas moves through the divergent section, it loses enough energy to reach atmospheric pressure and speeds up, even more, to go beyond the speed of sound. Inside the nozzle, gas dynamics are used to create supersonic flows. The main goal is to maximise thrust and get a better coating quality.

CGDS is used in various areas (such as aerospace, turbine, etc.,), those areas require less porosity of the coating. Due to less porosity coating adhesive strength is better, this is considered one of the advantages of cold-spray (CS) coating. But, in biomedical applications, porosity is desired up to certain levels. There were some studies that enhanced porosity levels by changing other parameters. Vilardell et al. [95] produced a highly porous and high surface roughness coating of pure Ti through the CS method by using coarse powder particles rather than spherical fine particles. Due to the large size of the particles, it decreased the velocity of particles which created large gaps in the deposition of coatings. This was beneficial in improving cell proliferation and osseointegration and showed better mechanical properties than the sand-blasted surface.

However, some studies have created porosity using magnesium or aluminium. Sun et al. sprayed Mg + Ti powders onto Ti to create porous coatings [96]. After being coated, the magnesium operated as a spacer but was removed by vacuum sintering. The pores in plasma-sprayed porous Ti coatings are not uniformly distributed and tend to lack good interconnectivity. Low porosity (37%), weak cohesion, and less binding strength are also characteristics of plasma spray. However, Mg and Ti CS coatings averaged 48.6% porosity and pore diameters of 70–150 µm. The porous Ti covering had bending and compressive Young's modulus that were similar to those of bone, suggesting that it might mitigate stress shielding to some degree. When compared to other coatings, CS coating has performed better in terms of biocompatibility and antibacterial surface [97]. In Table 5, different types of coatings and coating methods were discussed.

5.5 Friction Stir Processing

In friction stir processing (FSP), the surface of a material is modified using a rotating cylindrical instrument with a small pin. While applying an appropriate load, the tool is inserted and pushed along a desired length in the transverse plane. This generates significant plastic deformation and dynamic recrystallization of the material in the agitation region, resulting in the refinement of its microstructure [98]. FSP is mostly preferred to enhance corrosion properties, for instance, a study revealed that the elimination of porosity through densification can result in the prevention of pitting corrosion, which is commonly caused by an enlarged surface area [99]. Another study observed that particle refining effects were largely responsible for enhancing corrosion resistance. Smaller grain sizes, which are typically attained through FSP, tend to improve corrosion resistance by fostering Cr enrichment in the passive film [100].

FSP is favoured in certain unique scenarios, particularly when temporary implants made from degradable materials are utilised. Sampath et al. [41] studied AZ31 composite implants with polycaprolactone (PCL) and HA coating using FSP. On the substrate, a groove containing HA was distributed using a pin tool as shown in Fig. 10. The bioactivity of the sample was enhanced by the fine-grained matrix containing HA. In another study surface texture was created on EZ33A Mg alloy using FSP, this helped uniform degradation of Mg and this helped in increasing cell viability [101].

Table 5 Coated material systems and their properties of biomaterial

References	Coating/reinforcement	Substrate	Method	Mechanical properties	Observations
Singh et al. [88]	Ha-Nb	Mg alloy (ZK60)	Plasma spray	i. Nb-650 HV ii. HA-230 HV iii. HA-10%Nb-240 HV iv. HA-20%Nb-255 HV v. HA-30%Nb-270 HV	Higher Nb thermal conductivity led to a slower cooling rate in HA zones, which helped to form more brittleness
Abhijith et al. [146]	TiNbMoMnFe	304L SS	HVOF	i. 720 ± 3 $HV_{0.5}$ (milling time 5 h) ii. 871 ± 5 $HV_{0.5}$ (10 h) iii. 1021 ± 2 $HV_{0.5}$ (15 h)	The wettability and surface hardness of the coating increased The corrosion rate decreased while increasing the milling time of powders
Wang et al. [147]	Tantalum	TiO_2 nanotubes	Plasma spray (Thickness 100–300 nm)	–	An increase in surface roughness and hydrophilicity was observed Coating helped for enhancing osteogenic activity
Ebrahimi et al. [89]	HA and HA/Al_2O_3 &SiO_2	Pure Ti	Plasma spray	i. HA coating 420 HV ii. HA/Al_2O_3 &SiO_2 coating 390 HV	Bi-layer coating improved roughness and wettability Microhardness decreased due to an increase in porosity and large grain size Bi-layer coating improved cell viability and proliferation by up to 90% in 72 h
Stübinger et al. [148]	Ti/HA bilayed coating	Polyether ether ketone (PEEK)	Plasma spray	i. Surface roughness 30 ± 3 µm ii. Porosity 56%	Higher bone-to-implant contact rates compare to a single-layer and uncoated Coated implants showed better osseointegration
Sathish et al. [91]	YSZ Al_2O_3–13 wt%TiO_2 Bilayered	Ti–13Nb–13Z	Plasma spray	i. 617 ± 25 HV ii. 820 ± 22 HV iii. 1096 ± 10 HV	The lowest corrosion rate is shown in bilayer coating (0.0005 mm/yr) High porosity in Al_2O_3–13 wt%TiO_2 coating due to higher melting point of alumina
Xiao et al. [149]	FeCoNiCrMn	304 Stainless steel	Plasma spray	Hardness 273 ± 20 HV	Increasing H_2 flow rate, there was a change in microstructure, wear resistance and microhardness Mn and Cr elements formed oxides compared to other elements
Tüten et al. [150]	*TiTaHfNbZr*	Ti6Al4V	Magnetron sputtering	i. Uncoated 3.46 ± 0.17 GPa ii. HEA-coated 12.51 ± 0.34 GPa	The coating is produced with a fine-grain amorphous structure Coating enhanced mechanical properties (hardness and elastic modulus)
Meghwal et al. [151]	*AlCoCrFeNi*	Stainless steel	HVOF	i. HEA coating 7 ± 0.6 GPa ii. SS316L 3 ± 0.1 GPa	The HEA-coated sample showed superior corrosion resistance than SS316L Due to pitting corrosion interconnected micro-pits converted into larger holes in Al-Ni-rich regions

Table 5 (continued)

References	Coating/reinforcement	Substrate	Method	Mechanical properties	Observations
Ahn et al. [152]	CoCrFeMnNi	Low alloy steel	CS	i. HEA coating 423 HV ii. Heat treated at 550 °C is 399 HV iii. Heat treated at 850 °C is 220 HV	CS HEA coating showed ultra-fine grains H850 °C grains fully recrystallized (2.35 µm) resulted in a decrease in hardness values
Peighambardoust et al. [153]	$Ti_{1.5}ZrTa_{0.5}Nb_{0.5}Hf_{0.5}$	SS 316L Co–Cr–Mo Ti6Al4v	Magnetron sputtering	Vickers hardness values of three substrates after coating i. 11.43 GPa ii. 11.49 GPa iii. 11.45 GPa	SS316L and Co–Cr–Mo implants showed pitting corrosion while Ti alloys did not show any pitting signs. But, more corrosion resistance is shown in Co–Cr–Mo
Liu et al. [85]	$Fe_{25}Co_{25}Ni_{25}Al_{10}Ti_{15}$	Ti6Al4V	Magnetron sputtering	–	HEA coating reduced the dry friction coefficient by 37% Porous structure of T64 helped to accommodate friction particles which helped to absorb impact energy Increasing porous size helped to reduce the friction coefficient up to pd 30 µm
Henao et al. [77]	HA-TiO_2	Ti-6Al-4V	HVOF	–	Coating showed more stable electrochemical behaviour than uncoated Porosity of the coating helped to form a bone-like apatite structure after 7 days of immersion in SBF
Sun et al. [96]	Ti -Mg	Ti	CS	Porous size 70–100 µm	Porous Ti coating helped to reduce stress shielding around the bone
Lynn et al. [154]	HA	Ti-6Al-4V	Plasma spray	–	Up to 100 µm of HA coating thickness does not affect fatigue resistance of Ti-6Al-4V substrate Residual stresses did not vary while increasing coating thickness
Sampath et al. [41]	PCL/HA	AZ31	FSP	–	CaP coating reduced the degradation rate of AZ31 alloy The controlled degradation made the surface stable and conducive to cell adhesion and proliferation
Shunmugasamy et al. [101]	–	EZ33A Mg alloy	FSP	Corrosion rate up to 1 mm/year up to 8 weeks after that 0.7 mm/year next 4 weeks	FSP grain refinement, uniformly distributed secondary phases and preferred basal texture inhibit the corrosion process FSP results showed more uniformity of corrosion in Mg alloys Steady release of Mg ions aids implant-bone interface development

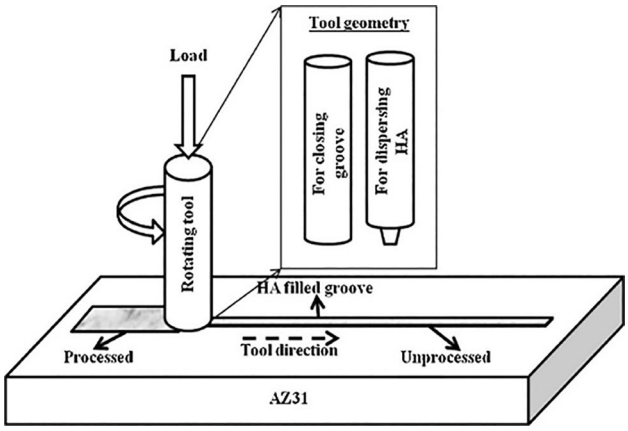

Fig. 10 Schematic representation of HA dispersion in AZ31 using FSP [41]

5.6 Laser Surface Texturing

LST has developed into a potent tool for obtaining the required functionality in existing materials; it is a one-step procedure for producing customised patterns on a small layer without changing any bulk characteristics of the material surface. The surface material of a substrate can be locally removed by exposing it to a laser emission of the right wavelength and fluence to create structures on the micron- or nano-size scale or both as shown in Fig. 11. As a result, the material undergoes modification in its surface energy, surface roughness, wettability, oxidation (passivation), porosity, and tribological characteristics [102]. Due to this outcome of LST, it became a more popular tool in biomedical applications. Micro-textures on implant surfaces may also significantly affect the tribological performance of contact surfaces, according to engineering studies. Surface topography was believed to be an important factor in how well orthopaedic and dental implants work, this was found by several studies [103, 104]. Surface topography is very important for osseointegration, and it is recognized that the surface texture of an implant can be attributed to how cells/tissue respond. Texturing the surface of metal-on-metal hip replacements has a potentially beneficial effect on reducing the asperity contact ratio and improving lubrication performance [105].

Many researchers around the world are studying the effects of different texture shapes and different ways to make textured surfaces. This is because textured implants with more surface area can make better bone-to-implant contact. Kedia et al. [79] studied cell adhesion and corrosion resistance of nanosecond laser-textured SS 316L. Experiments were conducted with four different laser powers 10, 50, 100, and 200 mW. Sample textured at 200 mW power had higher surface roughness (R_a 0.45 µm) but higher corrosion resistance due to a dense oxide layer that reduced defect density. It was observed that all specimens showed a superhydrophobic nature but 200 mW power specimen showed a more superhydrophobic nature due to more surface roughness, air trapped in microstructures and it did not allow water droplets to spread on the surface. Due to high laser power grooves formed wider in the 200 mW power textured sample which helped tissue cells to settle in grooves and spread to a larger area. Another study used numerical analysis of texturing to find an effect of lubrication to reduce wear debris on hip implants [105]. This study results showed simple cylindrical dimples showed better results in steady and transient

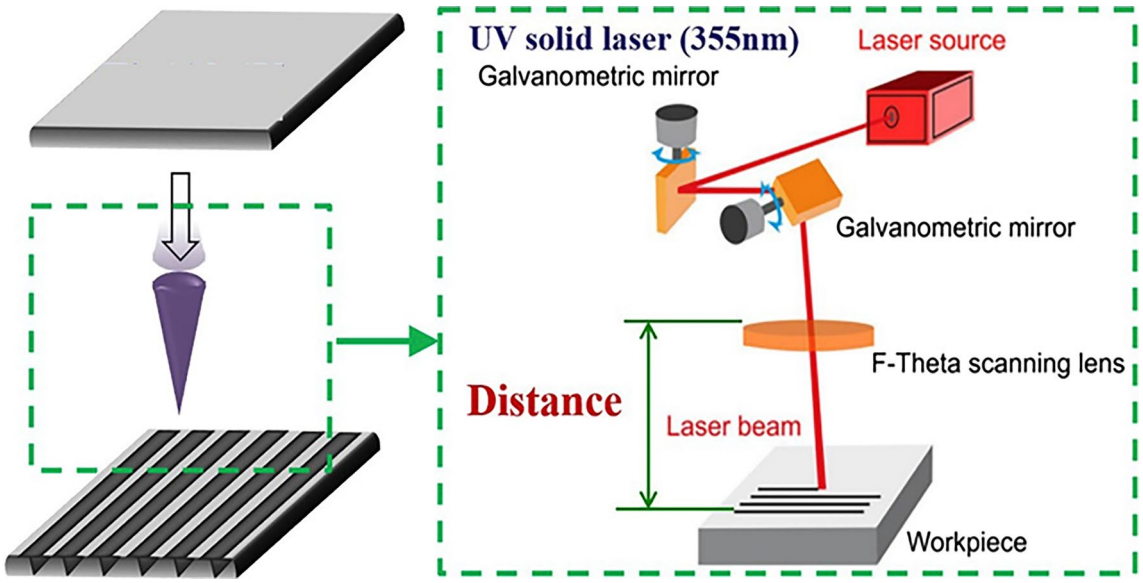

Fig. 11 Schematic diagram of laser surface texturing [167]

load conditions. Under boundary lubrication conditions, asperity contact ratio of the dimple surface (16%) was very less than smooth surface (58%), so dimple surface showed double improvement in lubrication compared to a smooth surface which helped to reduce friction pressure at joints on the hip implants.

Thus, by modifying the texture design parameters, a prosthetic hip implant could be optimised for the anatomy, body mass, and lifestyle activities of individual patients. Wettability is attribute of biomaterials because it makes tissue bond with the implant strong, which leads to better health of the tissue [106]. Surgeons could create a personalised medicine decision matrix that takes into account the texture design parameters of a prosthetic hip implant in addition to the size and materials of the implant for each patient. Lutey et al. [107] textured surfaces of spikes, laser-induced periodic surface structures (LIPSS), and nanopillars introduced those surfaces to *S. aureus* and *E. coli* bacteria compared those results with mirror polished surfaces as shown in Table 6. This study found that small textured surfaces (which are lesser than cell size) lessen the interaction region between bacteria and metal surface, help in the restriction of biofilm formation, and textured surface peaks induce bacteria to strain, which leads to the rupture of bacteria. Therefore, neither extremely low surface roughness nor super hydrophobicity alone is sufficient for minimising bacterial retention over different cells. Table 7 summarises the effect of laser surface texturing on different types of tissue cells.

5.7 Anodizing

The process of surface anodization generally involves the utilisation of an electrolyte solution, regulation of temperature and voltage, and the combination of both a cathode and an anode surface in order to get the desired outcome. Additionally, this treatment has the potential to be integrated with acid etching, sandblasting, or machining techniques. Significantly, a majority of studies employ the practice of mixing it with acid etching to facilitate the growth of oriented nanotubes or with polished surfaces [108].

When implemented at the nanoscale, this process has demonstrated exceptional outcomes in enhancing osseointegration within a timeframe ranging from one to two months. In a study, anodized SS 316L showed high impact strength (42 kJ/M^2) with an increment of 450% [109]. However, on the anodized surface cracks, shallow holes and oxidation formation were observed.

5.8 Sol–Gel

The sol–gel process is a wet-chemical method employed for crafting both glassy and ceramic materials. These thin film coatings are intended to increase surfaces' resistance to oxidation and wet corrosion. Recently, interest in sol–gel coatings has increased, with a particular emphasis on hybrid organic–inorganic variants. Ormosils are a class of organic–inorganic hybrid materials produced by the sol–gel method, which involves the hydrolysis and condensation of organically modified silanes in conjunction with traditional alkoxide precursors. In a research study, a sol–gel coating was applied to SS 316L using a mixture of tetraethyl orthosilicate (TEOS) and 3-methacryloxypropyltrim-ethoxysilane (TMSM). This application resulted in an increase in corrosion resistance, especially with higher TMSM content, attributable to the coating's increased flexibility [110].

5.9 Alkali Treatment

Alkali treatment is a process in which an alkaline solution is used to modify the properties of a substance. It is a common technique for improving the mechanical and thermal properties of natural fibres. By removing the cellulosic material that covers the external surface of the fibre's cell wall, this treatment improves the surface roughness and cellulose content exposed on the fibre surface. Consequently, it results in enhanced mechanical interlocking [111].

Table 6 Impact of implant surface properties on antibacterial properties [137]

Implant surface	Wettability (WCA)	Nature of surface	Surface roughness (nm)	Bacteria	
				S. aureus	*E. coli*
Untreated surface	–	–	370 ± 40	No reduction	No reduction
Mirror polished surface			31 ± 5	82.4% reduction	Bacteria cells doubled
Spikes (pulse energy 19.1 µJ)	160°	Superhydrophobic	8600 ± 100	69.8% reduction	Bacteria cells tripled
Laser-induced periodic surface structures (LIPSS) (pulse energy 1.01 µJ)	i. 119° ii. 26° (Treated with hot water at 90 °C for 48 h)	i. Hydrophobic ii. Hydrophilic	90 ± 5	i. 84.7% reduction ii. –	i. 99.8% reduction ii. 98.5% reduction
Nanopillars (pulse energy 1.46 µJ)	130°	Hydrophobic	60 ± 5	79.9% reduction	99.2% reduction

Table 7 Effect of laser surface texturing on different tissue cells (in vitro & in vivo analysis)

References	Laser parameters	Dimple size	Tissue cells	Observations
Mirhosseini et al. [155]	Pulse energy-100 MJ Frequency-10 HZ Wavelength-1064 nm	Diameter 156, 214, 127 µm	2T3 osteoblast cells	More cell growth percentage was observed in small-size patterns (127 µm) It found that optimum surface roughness for cell growth, and roughness closer to cell size improved cell growth Cells were uniform and evenly spread across patterns compared to untreated surfaces Untreated samples showed higher wettability than patterned surfaces
Mukherjee et al. [156]	Frequency 1000 HZ Wavelength 50–85 µm Scanning speed 50–80 mm/s Duty cycle 60–80%	Depth 60–65 µm	MG 63	At the same wavelength by reducing duty cycle, wider peaks were formed and at same duty cycle by reducing wavelength sharp peaks were formed It was observed that samples with similar avg. roughness, contact angle, and protein adsorption also showed different cell viability
Mesquita-Guimaraes et al. [157]	Power-25 W Velocity-200 mm/s frequency-550 Hz	$50 \times 50\ \mu m^2$ width 100 µm Depth 0, 40, 80 µm	MC3T3-E1 osteoblast cells	Laser micro-textured surface showed a 40% increase in cell viability compared to polished surface Optimal pattern size should be 100 to 200 µm, showing 60% more cell viability The most extensive cell layer formation was found on the laser-sintered HAp and 45S5 BG coatings, also by the cell viability values
Purnama et al. [158]	Pulse energy (E)-30, 40, 50 µJ Scan speed (v)-39, 59, 78, 97 mm s^{-1} Wavelength-1064 nm	Distance between patterns 25, 75, 150 µm	Endothelial cells (HUVECs) avg. size 25 µm	The adhesion of HUVEC cells is influenced by chain-like structures, which were introduced by laser structuring Due to laser treatment, some amount of iron hydroxide and impurities showed in the chemical composition analysis Adhesion, cell proliferation, and alignment of cells were significantly more in d25 surface compared to the remaining surfaces The optimal design condition was a pattern size closer to the size of a cell

In summary, there were various surface modification approaches expended for implants, in that thermal spray coatings, were widely used on account of their wide range of expedient outcomes. Among these, plasma spray is mostly preferred coating for biomedical applications. But, compared to plasma coatings, CS coatings exhibited better results against bacterial infections and corrosion. The literature showed that CS coatings are still in a nascent stage in biomedical applications. But, in other areas, these were promising choices for coatings due to low-temperature processing, this property of CS is very obliging for HEAs coating. In addition, FSP also showed good potential against corrosion and the method is preferred for temporary implants. Further, creating texturing on implant surfaces using LST improved the antibacterial and tribological properties of implants.

In conclusion, a wide range of surface modification methods have been employed for implants, with thermal spray coatings being particularly popular because of their range of metals and non-metals. Plasma spray coatings are frequently the preferred choice for biomedical applications. However, CS coatings have proven to perform better than plasma coatings in terms of resisting bacterial infections and corrosion. The literature shows that CS coatings are just starting to be used in biomedical uses. Despite this, they have demonstrated potential in various industries, primarily as a result of their low-temperature processing, which makes CS particularly beneficial for HEAs coatings.

FSP, which is used for temporary implants, has also shown substantial potential in preventing corrosion. Additionally, implants' antibacterial and tribological properties have been improved by modifying texture of implant surfaces using LST.

6 Essential Properties for Superior Functionality of Implant

Implant functionality includes a material's capacity to carry out its intended function within a human body effectively and efficiently. The various functions of an implant are illustrated in Fig. 12. The main objective is to improve or restore an organ or tissue's normal function. This requires responding to healing and ensuring long-term stability while integrating seamlessly with the surrounding tissues. The functionality of an implant is affected by a number of factors, including biocompatibility, mechanical strength, durability, and suitable design. Implant innovation continues to advance, leading to better patient outcomes, higher quality of life, and higher implantation operation success rates.

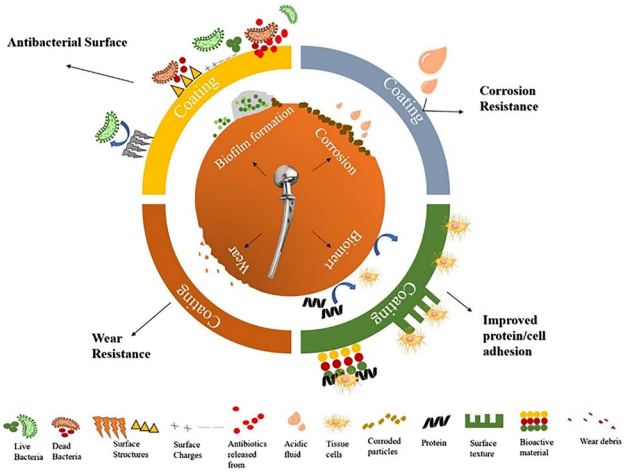

Fig. 12 Role of coating and surface modifications in challenging metal implant complications

6.1 Biocompatibility

Biocompatibility is the property of biomaterial to align with living cells without harming or causing further reactions. In terms of biocompatibility, the tissue reaction to the implant and the possibility of metal degradation within the body are two crucial factors. Bioactive materials are best for implants because these help to grow bone around them [15]. One concern regarding biocompatibility is thrombosis, which occurs when blood clots and platelets adhere to the surface of a biomaterial. Additionally, when a biomaterial is implanted in soft tissue, it can lead to the formation of fibrous tissue encapsulation [63].

Implants with poor biocompatibility resulted in tissue discolouration and eventually deterioration of a prosthetic joint, necessitating early replacement. Ti and its alloys are commonly utilised in endoprosthesis implants, in preparation of these implants a dense and stable layer of titanium dioxide (TiO_2) is coated on the base alloy. This protective layer ensures that the surrounding tissue does not come into direct contact with the metal surface, only interfaces with the oxide layer [112]. Iijima et al. compared bio HEAs ($Ti_{28.33}$ $Zr_{28.33}$ $Hf_{28.33}$ $Nb_{6.74}$ $Ta_{6.74}$ $Mo_{1.55}$) to traditional alloys used in biomedical applications and found that the HEAs performed as well as or better than pure Ti in terms of cell density [113]. A cell density of almost 7000 cells/cm^2 was reported for $Ti_{28.33}$ $Zr_{28.33}$ $Hf_{28.33}$ $Nb_{6.74}$ $Ta_{6.74}$ $Mo_{1.55}$. Ishimoto et al. reported 8000 cells/cm^2 cell density in SLM-HEA $Ti_{1.4}$ $Nb_{0.6}$ $Ta_{0.6}$ $Zr_{1.4}$ $Mo_{0.6}$ which was greater than 7500 cells/cm^2 for a casted alloy of the same composition, osteoblasts cell density on different samples are shown in Fig. 13 [114].

A porous, bioactive surface created by chemical and mechanical treatment increases the bone-to-implant interaction region without bone cement. Bhardwaj et al. reported

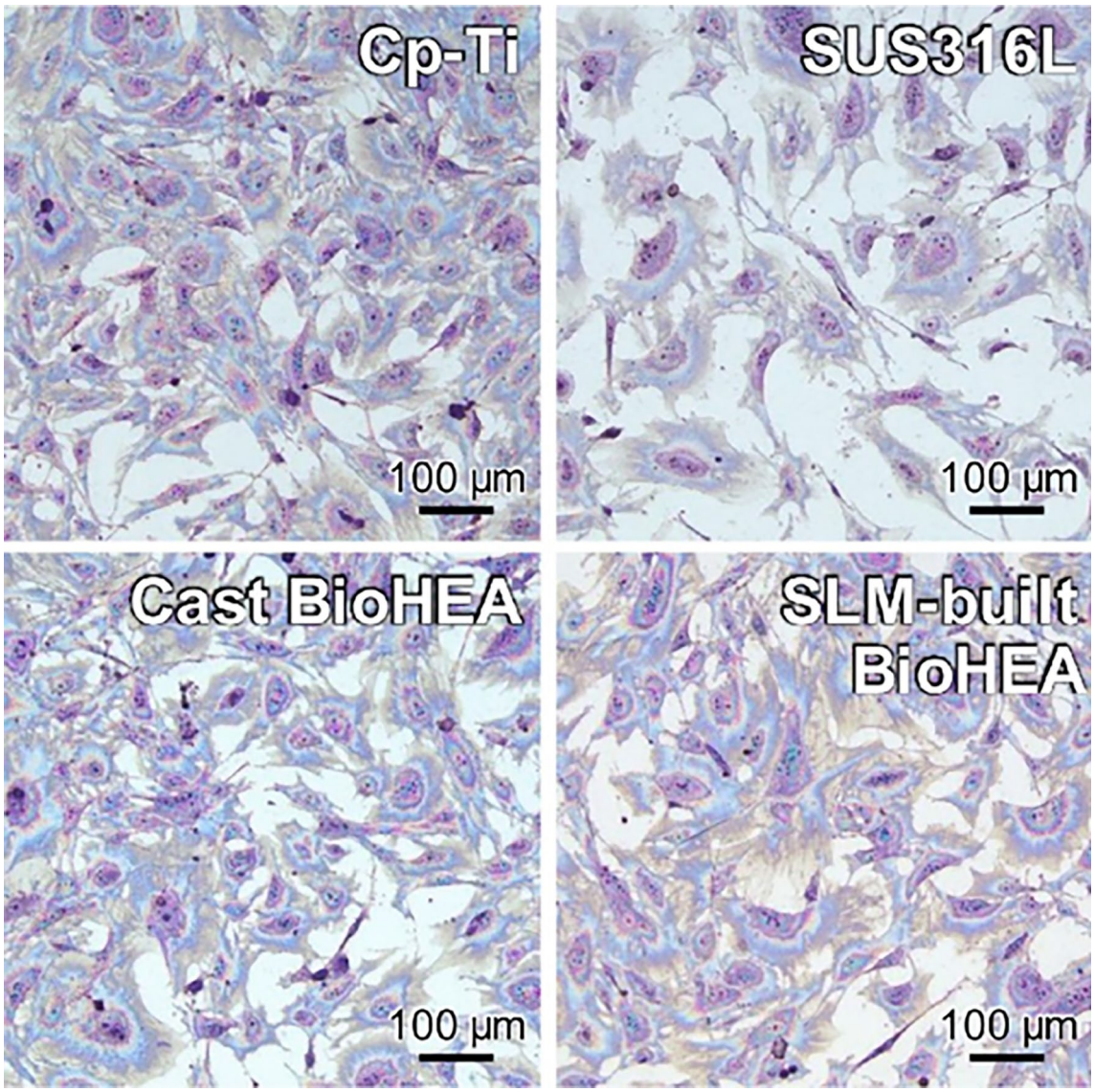

Fig. 13 Images of Giemsa-stained osteoblasts incubated on SLM-fabricated specimens, CP-Ti, SS 316L, and cast Bio-HEA counterpart [114]

that pore size does not affect tissue formation whereas less average pore size (13 μm) increased cell density [115]. Which helped to increase cell–cell interactions and to decrease apoptosis (death of cells). Addressing the issue of limited bioactivity upon implantation has presented a significant and challenging obstacle. As a result, researchers have developed surface treatments that involve applying coatings of bioactive materials to substrates. These treatments aim to enhance the bioactivity of the host tissue.

6.2 Antibacterial Surface

A surface that has been treated or created to prevent bacterial growth and proliferation, colonization, and the development of biofilms is referred to as an antibacterial surface. Surfaces with antimicrobial or anti-infection properties consist of various elements, including metals (silver, copper, zinc, zirconium, etc.), non-metal elements (selenium), organic chemicals (anti-infective peptides, antibiotics, chitosan, etc.,), and mixes thereof. When developing antimicrobial surfaces, factors such as ion-release surfaces resistant to bacteria, and surfaces capable of killing bacteria upon contact need to be taken into account. Peri-implantitis and implant failure can occur due to bacterial adhesion and colonization, facilitated by biofilm formation. The supplementation of magnesium reduces formation of biofilm and peri-implantitis [116].

Copper ions are used in a wide variety of modern medicinal and hygiene products for their antimicrobial properties. Copper and copper oxide are getting more and more attention because of their low toxicity, wide range of uses, and

affordable. Further, copper has antifouling properties also, as claimed by one of the studies that bacteria cells with CuO nanoparticles attached showed an increase in internal oxidative stress due to the generation of reactive oxygen species (ROS) [117]. Data found from the study indicated that the antifouling capabilities of a material are directly related to the surface microstructure. Thus, it was possible to prevent microbial attachment by controlling the surface's microstructure in Table 8 showed Cu antimicrobial properties. Zhang et al. studied the copper clusters (CuCs) effect on drug-resistant bacteria for instance Staphylococcus aureus (*S. aureus*) and *Pseudomonas aeruginosa* [118]. CuCs efficiently inhibited the bacteria growth on the surface of the implant, evidenced through SEM the death of bacteria was observed. As the amount of CuCs in the water rose, the bacterial wall and membrane slowly lost their shape. The walls and membranes of bacteria treated with CuCs were severely damaged and broken structures had a lot of Cu, which suggested that CuCs killed the bacteria. Moreover, compared to Ag clusters and Pt clusters produced with theanine peptide, wherever, CuCs demonstrated extremely low cytotoxicity. At high concentrations (400 µm), CuCs did not impose any toxicity on normal mammalian cells but, killed bacteria at lower concentrations (200 µm).

Gao et al. produced HEA CoCrFeCuNi with two different methods (SLM and traditional metallurgy) and tested them against Escherichia coli bacteria [119]. Cu ions released in SLM method were 25 and 12 mg/l in the traditional method, this resulted in cell viability of 98 and 94%, respectively, in the methods. Ren et al. [120] studied the antibacterial mechanism of 304 Cu containing stainless steel, to provide SS antibacterial properties, a surplus Cu element was added. The over-saturated Cu ions precipitated in the steel matrix and formed Cu-rich phases after the ageing solution, this offered SS antibacterial properties. Another study observed that large amounts of Cu precipitated on the passive layer, which helped to release more Cu- ions that could be dissolved on the surface of antibacterial stainless steel, giving it excellent antibacterial properties [121]. The antibacterial property was imparted owing to the great reduction ability of Cu- ions to take electrons from bacteria, causing their cytoplasm to flow off and cell nuclei to become oxidised, causing the death of the bacteria as shown in Fig. 14. Champagne et al. used plasma spray, wire spray, and CGDS to deposit copper on aluminium [97]. Observed the differences in microbiology and lowered the danger of infection from bacteria on touch surfaces like hospital tables. Due to the high number of dislocations in the coating, CGDS had the lowest amount of MRSA (*methicillin-resistant staphylococcus aureus*).

Table 8 In vitro experimental study about Cu antimicrobial property examined under Nikon Eclipse ME600 microscope

References	Name of microorganism	Time taken to kill microorganisms (bacteria)
Wilks et al. [159]	*Escherichia coli* O157 (bacteria)	90–270 min in 20 and 4 °C
Wilks et al. [160]	*Listeria monocytes* (bacteria)	No live bacteria were found after 60 min at room temperature
Noyce et al. [161]	Methicillin-resistant *Staphylococcus aureus* (MRSA) (bacteria)	A complete kill of bacteria in 45–90 min at room temperature at 4 °C within 6 h
Noyce et al. [162]	Influenza A virus	On Cu sample 2×10^6 virus particles were incubated after 24 h, 5×10^5 virus particles were observed

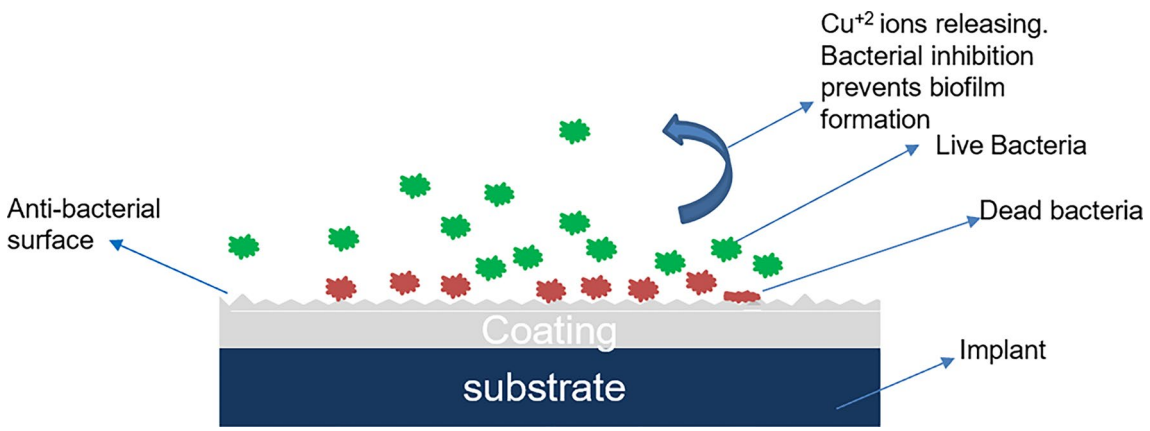

Fig. 14 Mechanism of killing bacteria by antibacterial-coated surface

6.3 Anticorrosive

An anticorrosive surface is designed to prevent the formation of corrosion on implants when exposed to biological and chemical environments. If a biomaterial does not have a permanent protective coating on its surface, corrosion will eventually eat through it. Biomaterials such as stainless steel, cobalt–chromium, Ti and its alloys, composites, and polymers experience corrosion on their exposed surfaces. For instance, metals may corrode when exposed to air, electrical stimulation, or bacteria-like foulants. Even though polymers can corrode in some situations, to prevent corrosion these can be coated with metallic powders. However, care must be taken while selecting a protective material, such as conducting polymers with conjugated carbon chain structures, which are powerful oxidants to the surface of the metal [122].

In this regard, it is suggested that new alloys be created by integrating nobler metals into stainless steel, Ti, and their alloys. The increased chromium and molybdenum content of the new class of super austenitic stainless steels renders them more passive, hence enhancing their corrosion resistance. To avoid Ni toxicity, Ni-free SS are proposed and explored for use in implant applications. Since niobium is more biocompatible and less expensive than vanadium, V-free Ti alloys, such as Ti-6Al-7Nb alloy, have been created for improved corrosion and wear resistance in orthopaedic implants [123]. For high-temperature applications, thermal spraying techniques such as D-gun, atmospheric plasma spray (APS), and HVOF have been widely employed to apply corrosion-prevention coatings of nickel, tantalum, chromium, tungsten carbide, and their alloys. In a study, HA was coated on Ti6Al4V through HVOF coating it improved corrosion resistance (0.00164–0.000975 mA/cm^2) [77].

6.4 Wear Resistant

The earlier discussion demonstrates the importance of wear resistance of an implant for its proper functionality. Several investigations into the tribological properties of developed biomaterials need to be conducted before testing it as an implant. Wear on biomaterials is predominantly contributed by oxidational wear. In the process of rubbing metals a contacting asperity removes the native oxide layer. Consequently, an oxide layer forms on the metal surface, acting as a barrier that prevents ion movement between the metal and the surrounding environment, thereby inhibiting corrosion. However, the wear of the implant can compromise this protective layer. Once the layer is compromised, corrosion protection is lost, and the metal is exposed to corrosion. Additionally, another concern arises as the worn debris from the implant can trigger an immune system response, resulting in inflammation and aseptic loosening [67].

In orthopaedics and dentistry, Ti and its alloys are frequently utilised. However, the long-term use of Ti for implants poses challenges due to the weak tribological characteristics of Ti-based alloys [124]. Similar issues arise when employing SS 316L or Mg alloys for bone restoration, as they exhibit low resistance to wear and corrosion. Given the significance of wear resistance to the longevity of implants within the human body, research is currently underway to improve performance by developing surface coatings.

Kusinski et al. [125] improved the wear resistance of knee replacement implants with CGDS of Ti/TiC on Ti alloy. Low porosity, high bond strength (21 MPa) and homogeneity of TiC particles in the Ti matrix were observed in the coating. TiC-coated particles decreased COF and rate of wear (which was less than Ti and SS) because of carbide particle hardness (850 HV). In another study, HEA (FeCoNiTiAl) coating was done on Ti6Al4V using magnetron sputtering to enhance the wear resistance of artificial joints by Liu et al. [126]. The porous effect on wear and coefficient of friction was discussed in this study, the substrate was mixed with $CO(NH_2)_2$ with different sizes of particles (Pd 10 and 30 µm) with pressurising and sintering processes porous substrate created. HEA coating reduced 50% coefficient of friction (COF) compared to uncoated Ti6Al4V. The porous structure helped to hold wear particles up to some size of porous structure but, in large pore size (Pd 30 µm) sample showed more wear due to higher surface roughness led to more removal of material. Due to pores coating stress shielding in implants effectively decreased but, large pores size was also not helpful for wear-resistant coating.

The properties listed above play an important role in improving the effectiveness of implant surfaces, and having such properties in an implant helps to its potential to control toxicity in the human body. Several researchers have expressed a preference for refractory metals to improve these properties. However, when it comes to antibacterial properties, researchers regularly chose copper over silver and zinc due to its ease of availability and efficiency against bacteria. A biocompatible HEA (Bio-HEA) that is minimal in toxicity to the human body. According to published research, Bio-HEA made of refractory metals, copper, and a few other biomaterials, is anticipated to perform better and be safer than conventional metal implants. As seen in Table 9, there is a distinct difference between the qualities offered by the various coating types, with each coating serving a specialised function. When compared to conventional coatings, the elemental composition of HEAs, which are found in these alloys, enables these coatings to exhibit superior potential.

Table 9 Different purposes of coating on implants

References	Coating	Substrate	Method of coating	Purpose of coating	Observations
Hassan et al. [63]	Graphite	SS 316L	Physical vapour deposition (PVD) Coating thickness 15 ± 2–1009 ± 22 nm	Anti-corrosive, biocompatibility	The corrosion rate improved from 22 m/year to 1.4 m/year Surface roughness 0.004–0.001 µm. Microhardness 350 HV Due to graphite coating biocompatibility improved
Kumar et al. [163]	Ti-Baghdadite composite	SS 316L	CS Coating thickness 236 ± 11 µm	Anticorrosive and biocompatibility	Surface roughness and porosity of coating improved with increase in BAG composition A large improvement in corrosion rate was observed, uncoated substance (268 µm/year), and composite coating (0.154 µm/year) At 25% BAG composition coating observed cell viability at 120%
Singh et al. [28]	HA-TiO_2	Ti-35Nb-7Ta-5Zr	Plasma spray Coating thickness 185–200 µm	Anticorrosive and biocompatibility	Reinforcement of TiO_2 in HA improved microstructure and mechanical bonding of coating E_{corr} values of HA-TiO_2 (-420 mV) less than HA coating (-330 mV) improvement in corrosion resistance was observed After 7 days, cell density of reinforcement coating (53 cells/cm^2) was better than HA coating (35 cells/cm^2)
JunRong et al. [164]	Tantalum	Ti6Al4V	CS Max thickness 380 µm Min thickness 24 µm	Biocompatibility, and wear resistance	The rough and porous coating formed The Microhardness of the outer part of the coating is less than the inner part due to porosity Good bioactivity showed in the form of cell proliferation

Table 9 (continued)

References	Coating	Substrate	Method of coating	Purpose of coating	Observations
Henao et al. [77]	HA	Ti6Al4V	HVOF Four coating layers mean thickness of coating 350 ± 7 µm	Anticorrosive	Graded porosity was observed in the coating Corrosion resistance improved from (0.00164–0.000975 mA/cm^2) after coating The bioactivity of the implant increased after coating After 28 days, the bone-like apatite phase consolidated and sealed the graded coating's porosity
Zhao et al. [165]	Reductive graphene oxide-Ag nanoparticle-Al	Mild Steel	CS	Antibacterial	The coating showed high antibacterial properties against Escherichia coli Homogeneity of the coating was observed
Vilardell et al. [95]	Pure Ti	–	CS	Biocompatibility	High roughness (30–50 µm) and high wettability (WCA 28°) Higher cell viability and good cell proliferation
Al-Mangour et al. [166]	SS67%–Co33.3%	Mild steel	CS Coating thickness 0.5–3.4 mm	Anti-corrosive	SS-33%Co coating showed a better corrosion rate than SS coating Annealing (1100 °C) after coating improved densification and porosity reduction

7 Conclusion and Future Trends

This review examined implant surface characteristics such as surface texture, surface energy, and porosity, as well as implant failure occurrences. Improving orthopaedic implants' durability entails addressing challenges associated with corrosion resistance, wear resistance, and biocompatibility. Improving orthopaedic implants' durability entails addressing challenges associated with corrosion resistance, wear resistance, and biocompatibility. Numerous surface modification methods were investigated as prospective for enhancing these properties; each method discussed in this review was different from others, offering a variety in improving surface properties. The development of implant coatings is critical for reducing patient discomfort caused by metal debris.

Following are some conclusions made through this review:

1. Depending on the properties and uses, several rare earth elements, such as SS 316L, Co–Cr alloys, Ti alloys, and Mg, are employed as orthopaedic implant materials. Despite this progress, people continue to experience considerable difficulties after surgery.
2. Surface porosity within a diameter range of 100–700 µm can improve the interaction between tissue and implants. Furthermore, surface roughness of less than 1 µm encourages cell and tissue development within grooves. Excessive inhomogeneous surface roughness, on the other hand, promotes bacterial growth and biofilm formation.
3. The release of Al, Cr, and Ni metal ions from Ti alloys, SS 316L, and Co-Cr alloys owing to implant corrosion causes elevated levels of metal toxicity in the human body, which contributes to Alzheimer's, lung diseases, neurological effects, skin disorders, etc.

4. Thermal spray coatings have been widely used to modify the surface of implants because these can be used on a wide range of metals and non-metals. Among these, cold-spray coatings exhibited better resistance to bacterial infection and corrosion.
5. Metallic implants made from silver, copper, or zinc have been clinically shown to be highly effective against bacteria, with copper being the metal of choice for researchers due to its low cost, wide availability, and high effectiveness against bacteria.
6. Laser surface texturing has been found to improve wear and corrosion resistance. The trapped air in textured surface grooves aids in the prevention of microorganism colonization. The hydrophobic nature of the surface causes this, and texturing the surface promotes cell survival and density.

Researchers are focusing more and more on alloys instead of traditional biomaterials because even a small addition of a key element has shown that it can greatly improve the properties of biomaterials. Due to their low toxicity, researchers often selected refractory metals while making alloy mixtures. Also, the study showed that the released copper ions could break up bacterial membranes and stop their growth. This led to a lot of research on copper as an antibacterial surface.

In the biomedical area, the use of high entropy alloys (HEA) is still in its early stages. Nonetheless, given their practical advantages, HEAs could become the dominating materials in this industry in the future. According to the review study's findings, HEAs comprising a combination of group IV, group V, and antimicrobial elements (such as Ag, Cu, Zn, and so on) are expected to produce excellent outcomes.

Acknowledgements J Sharath Kumar thanks to Ministry of Education, Government of India for the research scholarship.

Declarations

Conflict of interest It is stated that there are no conflicts of interest to disclose.

References

[1] S. Santhosh Kumar, S.S. Hiremath, B. Ramachandran, V. Muthuvijayan, Biotribology **18**, 100095 (2019)
[2] L.Y. Chen, H.Y. Zhang, C. Zheng, H.Y. Yang, P. Qin, C. Zhao, S. Lu, S.X. Liang, L. Chai, L.C. Zhang, Mater. Des. **208**, 109907 (2021)
[3] H. Amel-Farzad, M.T. Peivandi, S.M.R. Yusof-Sani, Eng. Fail. Anal. **14**, 1205 (2007)
[4] S. Dittrick, V.K. Balla, N.M. Davies, S. Bose, A. Bandyopadhyay, Mater. Sci. Eng. C **31**, 809 (2011)
[5] Y. Kubota, T. Kuroki, S. Akita, T. Koizumi, M. Hasegawa, N. Rikihisa, N. Mitsukawa, K. Satoh, J. Plast. Reconstr. Aesthet. Surg. **65**, 372 (2012)
[6] A. Goharian, M.R. Abdullah, *Trauma Plating Systems* (Elsevier, 2017), pp.115–142
[7] B. Zhang, D. Myers, G. Wallace, M. Brandt, P. Choong, Int. J. Mol. Sci. **15**, 11878 (2014)
[8] Y. Abu-Amer, I. Darwech, J.C. Clohisy, Arthritis Res. Ther. **9**, S6 (2007)
[9] S.M. Kurtz, K.L. Ong, E. Lau, M. Widmer, M. Maravic, E. Gómez-Barrena, M. De Fátima Pina, Int. Ortho. **35**, 1783 (2011)
[10] ISHKS, Newsletter 2019. https://ishks.com/pdf/ISHKS-Newsletter-2019.pdf. Accessed 19 Sep 2023
[11] Y. Liu, B. Rath, M. Tingart, J. Eschweiler, J. Biomed. Mater. Res. A **108**, 470 (2020)
[12] J.M. Morais, F. Papadimitrakopoulos, D.J. Burgess, AAPS J. **12**, 188 (2010)
[13] T.Y. Liao, A. Biesiekierski, C.C. Berndt, P.C. King, E.P. Ivanova, H. Thissen, P. Kingshott, Prog. Surf. Sci. **97**, 100654 (2022)
[14] I. Ratha, P. Datta, V.K. Balla, S.K. Nandi, B. Kundu, Ceram. Int. **47**, 4426 (2021)
[15] R. Junker, A. Dimakis, M. Thoneick, J.A. Jansen, Clin. Oral Implants Res. **20**, 185 (2009)
[16] B. Priyadarshini, M. Rama, Chetan, U. Vijayalakshmi, J. Asian Ceram. Soc. **7**, 397 (2019)
[17] E. Mostaed, M. Sikora-Jasinska, J.W. Drelich, M. Vedani, Acta Biomater. **71**, 1 (2018)
[18] E. Zhang, H. Chen, F. Shen, J. Mater. Sci. Mater. Med. **21**, 2151 (2010)
[19] V. Tsakiris, C. Tardei, F.M. Clicinschi, J. Magnes. **9**, 1884 (2021)
[20] T. Odaira, S. Xu, K. Hirata, X. Xu, T. Omori, K. Ueki, K. Ueda, T. Narushima, M. Nagasako, S. Harjo, T. Kawasaki, L. Bodnárová, P. Sedlák, H. Seiner, R. Kainuma, Adv. Mater. **34**, 2202305 (2022)
[21] L. Patnaik, S. Ranjan Maity, S. Kumar, Mater. Today Proc. **26**, 638 (2020)
[22] M.Z. Ibrahim, A.A.D. Sarhan, F. Yusuf, M. Hamdi, J. Alloys Compd. **714**, 636 (2017)
[23] L.C. Zhang, L.Y. Chen, Adv. Eng. Mater. **21**, 1801215 (2019)
[24] S. Dutta, S. Gupta, M. Roy, A.C.S. Biomater, Sci. Eng. **6**, 4748 (2020)
[25] S. Engelhart, R.J. Segal, Cutis **99**, 245 (2017)
[26] J. Zhou, C. Liu, Y. Wu, L. Xie, F. Yin, D. Qian, Y. Song, L. Wang, L.C. Zhang, L. Hua, J. Mater. Sci. Technol. **25**, 5693 (2023)
[27] Y.W. Cui, L.Y. Chen, Y.H. Chu, L. Zhang, R. Li, S. Lu, L. Wang, L.C. Zhang, Corros. Sci. **215**, 111017 (2023)
[28] S. Singh, C. Prakash, H. Singh, Surf. Coat. Technol. **398**, 126072 (2020)
[29] D. Wu, R.M. Bhalekar, J.S. Marsh, D.J. Langton, A.J. Stewart, EFORT Open Rev. **7**, 758 (2022)
[30] X. Wang, K. Yeung, J.P.Y. Cheung, J.Y.N. Lau, W. Qi, K.M.C. Cheung, C.E. Aubin, Spine Deform. **8**, 369 (2020)
[31] L. Luo, A. Petit, J. Antoniou, D.J. Zukor, O.L. Huk, R.C.W. Liu, F.M. Winnik, F. Mwale, Biomaterials **26**, 5587 (2005)
[32] B. Singh, G. Singh, B.S. Sidhu, Surf. Coat. Technol. **377**, 124932 (2019)
[33] S.P. Wang, J. Xu, Mater. Sci. Eng. C **73**, 80 (2017)
[34] Y. Li, C. Wong, J. Xiong, P. Hodgson, C. Wen, J. Dent. Res. **89**, 493 (2010)
[35] A. Scarano, M. Piattelli, S. Caputi, G.A. Favero, A. Piattelli, J. Periodontol. **75**, 292 (2004)
[36] Y. Tsutsumi, Corros. Eng. **63**, 281 (2014)
[37] V. Sharma, S. Chowdhury, N. Keshavan, B. Basu, Int. Mater. Rev. **68**, 46 (2023)

[38] S. Affatato, N. Freccero, P. Taddei, J. Mech. Behav. Biomed. Mater. **53**, 40 (2016)
[39] M.V. Birman, P.C. Noble, M.A. Conditt, S. Li, K.B. Mathis, J. Arthroplasty **20**, 87 (2005)
[40] S.J. Meng, H. Yu, S.D. Fan, Q.Z. Li, S.H. Park, J.S. Suh, Y.M. Kim, X.L. Nan, M.Z. Bian, F.X. Yin, W.M. Zhao, B.S. You, K.S. Shin, Acta Metall. Sin. -Engl. Lett. **32**, 145 (2019)
[41] T.S. Sampath Kumar, G. Perumal, M. Doble, S. Ramakrishna, J. Mater. Process. Technol. **252**, 398 (2018)
[42] A. Purnama, H. Hermawan, J. Couet, D. Mantovani, Acta Biomater. **6**, 1800 (2010)
[43] H.R. Bakhsheshi-Rad, E. Hamzah, H.T. Low, M.H. Cho, M. Kasiri-Asgarani, S. Farahany, A. Mostafa, M. Medraj, Acta Metall. Sin. -Engl. Lett. **30**, 201 (2017)
[44] J.S. Kumar, C.V.S. Raju, A.B. Naik, R. Kumar, R. Verma, Surf. Topogr. **10**, 035027 (2022)
[45] B.S. Murty, J.W. Yeh, S. Ranganathan, P.P. Bhattacharjee, *High-Entropy Alloys* (Elsevier, 2019), pp.30–35
[46] N. Ma, S. Liu, W. Liu, L. Xie, Front. Bioeng. Biotechnol. **08**, 603522 (2020)
[47] C.S. Feng, T.W. Lu, T.L. Wang, M.Z. Lin, J. Hou, W. Lu, W.B. Liao, Acta Metall. Sin. -Engl. Lett. **34**, 1537 (2021)
[48] S. Gurel, M.B. Yagci, D. Canadinc, G. Gerstein, B. Bal, H.J. Maier, Mater. Sci. Eng. A **803**, 140456 (2021)
[49] S. Gurel, M.B. Yagci, B. Bal, D. Canadinc, Mater. Chem. Phys. **254**, 123377 (2020)
[50] J. Feng, Y. Tang, J. Liu, P. Zhang, C. Liu, L. Wang, Front. Bioeng. Biotechnol. **10**, 977282 (2022)
[51] R. Krishna Alla, K. Ginjupalli, N. Upadhya, M. Shammas, R. Krishna Ravi, R. Sekhar, Trends Biomater. Artif. Organs **25**, 112 (2011)
[52] M.P. Gispert, A.P. Serro, R. Colaço, E. Pires, B. Saramago, J. Biomed. Mater. Res. B Appl. Biomater. **84B**, 98 (2008)
[53] B. Jahani, Biomed. J. Sci. Tech. Res. **38**, 30058 (2021)
[54] S. Hansson, M. Norton, J. Biomech. **32**, 829 (1999)
[55] P.O. Cubillos, V.O. dos Santos, A.L.A. Pizzolatti, A.D.O. Moré, C.R.M. Roesler, J. Test. Eval. **49**, 20200357 (2021)
[56] B. Ren, Y. Wan, C. Liu, H. Wang, M. Yu, X. Zhang, Y. Huang, Mater. Sci. Eng. C **118**, 111505 (2021)
[57] D.W. Fabi, B.R. Levine, ASM Handb. Mater. Med. Devices **23**, 307 (2012)
[58] F. Matassi, A. Botti, L. Sirleo, Clin. Cases Miner. Bone Metab. **10**, 111 (2013)
[59] R. Singh, J.S. Sidhu, Rishab, B.S. Pabla, A. Kumar, J. Mater. Eng. Perform. **31**, 240 (2022)
[60] W. Yan, J. Berthe, C. Wen, Mater. Des. **32**, 1776 (2011)
[61] S. Wang, X. Zhou, L. Liu, Z. Shi, Y. Hao, Med. Eng. Phys. **81**, 30 (2020)
[62] R.A. Gittens, T. McLachlan, R. Olivares-Navarrete, Y. Cai, S. Berner, R. Tannenbaum, Z. Schwartz, K.H. Sandhage, B.D. Boyan, Biomaterials **32**, 3395 (2011)
[63] S. Hassan, A.Y. Nadeem, M. Ali, M.N. Ali, M.B.K. Niazi, A. Mahmood, Mater. Chem. Phys. **290**, 126562 (2022)
[64] A. Mishra, Acta Metall. Sin. -Engl. Lett. **30**, 326 (2017)
[65] K.L. Urish, N.J. Giori, J.E. Lemons, W.M. Mihalko, N. Hallab, Ortho Clin. **50**, 281 (2019)
[66] N.S. Manam, W.S.W. Harun, D.N.A. Shri, S.A.C. Ghani, T. Kurniawan, M.H. Ismail, M.H.I. Ibrahim, J. Alloys Compd. **701**, 698 (2017)
[67] P.A. Dearnley, Surf. Coat. Technol. **198**, 483 (2005)
[68] H.G. Willert, G.M. Brobäck, G.H. Buchhorn, Clin. Orthop. Relat. Res. **1**, 56 (1996)
[69] K. Van Gaalen, C. Quinn, F. Benn, P.E. McHugh, A. Kopp, T.J. Vaughan, Bioact. Mater. **21**, 32 (2023)
[70] C. Solá, A. Amorim, Á. Espías, S. Capelo, J. Fernandes, L. Proença, L. Sanchez, I. Fonseca, Int. J. Electrochem. Sci. **8**, 406 (2013)
[71] Y.W. Cui, L.Y. Chen, P. Qin, R. Li, Q. Zang, J. Peng, L. Zhang, S. Lu, L. Wang, L.C. Zhang, Corros. Sci. **203**, 110333 (2022)
[72] D.J. Blackwood, Corros. Rev. **21**, 97 (2003)
[73] N. Hafeez, D. Wei, L. Xie, Y. Tang, J. Liu, H. Kato, W. Lu, L.C. Zhang, L. Wang, Addit. Manuf. **48**, 102376 (2021)
[74] D.C. Hansen, Electrochem. Soc. Interface **17**, 31 (2008)
[75] G. Manivasagam, D. Dhinasekaran, A. Rajamanickam, Recent Pat. Corros. Sci. **2**, 40 (2010)
[76] L.C. Zhang, L.Y. Chen, L. Wang, Adv. Eng. Mater. **22**, 1901258 (2020)
[77] J. Henao, O. Sotelo-Mazon, A.L. Giraldo-Betancur, J. Hincapie-Bedoya, D.G. Espinosa-Arbelaez, C. Poblano-Salas, C. Cuevas-Arteaga, J. Corona-Castuera, L. Martinez-Gomez, J. Mater. Res. Technol. **9**, 14002 (2020)
[78] J. Liu, J. Liu, S. Attarilar, C. Wang, M. Tamaddon, C. Yang, K. Xie, J. Yao, L. Wang, C. Liu, Y. Tang, Front. Bioeng. Biotechnol. **8**, 576969 (2020)
[79] S. Kedia, S.K. Bonagani, A.G. Majumdar, V. Kain, M. Subramanian, N. Maiti, J.P. Nilaya, Colloid Interface Sci. Commun. **42**, 100419 (2021)
[80] X. Wei, W. Li, B. Liang, B. Li, J. Zhang, L. Zhang, Z. Wang, Tribol. Int. **97**, 212 (2016)
[81] A. Jemat, M.J. Ghazali, M. Razali, Y. Otsuka, Biomed. Res. Int. **2015**, 1 (2015)
[82] A. Gupta, N. Kumar, A. Sachdeva, Mater. Today Proc. (2023). https://doi.org/10.1016/j.matpr.2023.07.239
[83] L.Y. Chen, S.X. Liang, Y. Liu, L.C. Zhang, Mater. Sci. Eng. R **146**, 100648 (2021)
[84] X. Xu, Y. Lu, S. Li, S. Guo, M. He, K. Luo, J. Lin, Mater. Sci. Eng. C **90**, 198 (2018)
[85] D. Liu, Z. Ma, W. Zhang, B. Huang, H. Zhao, L. Ren, Tribol. Int. **158**, 106937 (2021)
[86] J. Singh, S.S. Chatha, H. Singh, Ceram. Int. **47**, 9143 (2021)
[87] R.B. Heimann, J. Therm. Spray Technol. **27**, 1212 (2018)
[88] B. Singh, G. Singh, B.S. Sidhu, N. Bhatia, Mater. Chem. Phys. **231**, 138 (2019)
[89] N. Ebrahimi, A.S.A.H. Zadeh, M.R. Vaezi, M. Mozafari, Surf. Coat. Technol. **352**, 474 (2018)
[90] W. Zórawski, A. Góral, O. Bokuvka, L. Lityńska-Dobrzyńska, K. Berent, Surf. Coat. Technol. **268**, 190 (2015)
[91] S. Sathish, M. Geetha, S.T. Aruna, N. Balaji, K.S. Rajam, R. Asokamani, Ceram. Int. **37**, 1333 (2011)
[92] V. Kumar, R. Verma, V.S. Sharma, V. Sharma, Surf. Topogr. Metrol. Prop. **9**, 043003 (2021)
[93] R.S. Lima, M.N. Bureau, J.G. Legoux, F. Chellat, R.S. Lima, B.R. Marple, M.N. Bureau, H. Shen, G.A. Candeliere, J. Therm. Spray Technol. **15**, 2006 (2006)
[94] M. Gaona, R.S. Lima, B.R. Marple, Mater. Sci. Eng. A **458**, 141 (2007)
[95] A.M. Vilardell, N. Cinca, N. Garcia-Giralt, S. Dosta, I.G. Cano, X. Nogués, J.M. Guilemany, J. Mater. Sci. Mater. Med. **29**, 19 (2018)
[96] J. Sun, Y. Han, K. Cui, Mater. Lett. **62**, 3623 (2008)
[97] A.M. Vilardell, N. Cinca, A. Concustell, S. Dosta, I.G. Cano, J.M. Guilemany, J. Mater. Sci. **50**, 4441 (2015)
[98] W. Wang, P. Han, P. Peng, T. Zhang, Q. Liu, S.N. Yuan, L.Y. Huang, H.L. Yu, K. Qiao, K.S. Wang, Acta Metall. Sin. -Engl. Lett. **33**, 43 (2020)
[99] M. Lotfollahi, M. Shamanian, A. Saatchi, Mater. Des. **62**, 282 (2014)
[100] Y. Zhao, C. Dong, Z. Jia, J. You, J. Tan, S. Miao, Y. Yi, Adv. Mater. Sci. Eng. **2021**, 1 (2021)

[101] V.C. Shunmugasamy, M. AbdelGawad, M.U. Sohail, T. Ibrahim, T. Khan, T.D. Seers, B. Mansoor, Bioact. Mater. **28**, 448 (2023)
[102] V. Kumar, R. Verma, S. Kango, V.S. Sharma, Mater. Today Commun. **26**, 101736 (2021)
[103] L. Tiainen, P. Abreu, M. Buciumeanu, F. Silva, M. Gasik, R. Serna Guerrero, O. Carvalho, J. Mech. Behav. Biomed. Mater. **98**, 26 (2019)
[104] J. Han, F. Zhang, B. Van Meerbeek, J. Vleugels, A. Braem, S. Castagne, Mater. Sci. Eng. C **123**, 112034 (2021)
[105] L. Gao, P. Yang, I. Dymond, J. Fisher, Z. Jin, Tribol. Int. **43**, 1851 (2010)
[106] M. May, E. Paul, C. Pavan Satyanarayana, L. Ratna Raju, B. Ratna Sunil, IOP Conf. Ser. Mater. Sci. Eng. **1185**, 012012 (2021)
[107] A.H.A. Lutey, L. Gemini, L. Romoli, G. Lazzini, F. Fuso, M. Faucon, R. Kling, Sci. Rep. **8**, 10112 (2018)
[108] D.J. Hall, R.M. Urban, R. Pourzal, T.M. Turner, A.K. Skipor, J.J. Jacobs, J. Biomed. Mater. Res. B Appl. Biomater. **105**, 283 (2017)
[109] S.A. Ibrahim, S.H. Lafta, W.A. Hussain, J. Mech. Behav. Mater. **30**, 272 (2021)
[110] S.M. Hosseinalipour, A. Ershad-langroudi, A.N. Hayati, A.M. Nabizade-Haghighi, Prog. Org. Coat. **67**, 371 (2010)
[111] T. Šoštarić, M. Petrović, J. Stojanović, M. Marković, J. Avdalović, A. Hosseini-Bandegharaei, Z. Lopičić, Biomass Convers. Biorefin. **12**, 2377 (2022)
[112] C. Wolner, G.E. Nauer, J. Trummer, V. Putz, S. Tschegg, Mater. Sci. Eng. C **26**, 34 (2006)
[113] Y. Iijima, T. Nagase, A. Matsugaki, P. Wang, K. Ameyama, T. Nakano, Mater. Des. **202**, 109548 (2021)
[114] T. Ishimoto, R. Ozasa, K. Nakano, M. Weinmann, C. Schnitter, M. Stenzel, A. Matsugaki, T. Nagase, T. Matsuzaka, M. Todai, H.S. Kim, T. Nakano, Scr. Mater. **194**, 113658 (2021)
[115] T. Bhardwaj, R.M. Pilliar, M.D. Grynpas, R.A. Kandel, J. Biomed. Mater. Res. **57**, 190 (2001)
[116] L. Ren, X. Lin, L. Tan, K. Yang, Mater. Lett. **65**, 3509 (2011)
[117] Y. Wu, W. Wu, W. Zhao, X. Lan, Surf. Coat. Technol. **395**, 125911 (2020)
[118] X. Zhang, Z. Zhang, Q. Shu, C. Xu, Q. Zheng, Z. Guo, C. Wang, Z. Hao, X. Liu, G. Wang, W. Yan, H. Chen, C. Lu, Adv. Funct. Mater. **31**, 2008720 (2021)
[119] J. Gao, Y. Jin, Y. Fan, D. Xu, L. Meng, C. Wang, Y. Yu, D. Zhang, F. Wang, J. Mater. Sci. Technol. **102**, 159 (2022)
[120] L. Ren, L. Nan, K. Yang, Mater. Des. **32**, 2374 (2011)
[121] L. Nan, W. Yang, Y. Li, M. Lu, Y. Liu, K. Yang, J. Mater. Sci. Technol. **24**, 197 (2008)
[122] K. Auepattana Aumrung, T. Phakkeeree, D. Crespy, Prog. Org. Coat. **163**, 106639 (2022)
[123] A.R. Rafieerad, A.R. Bushroa, B. Nasiri-Tabrizi, S.H.A. Kaboli, S. Khanahmadi, A. Amiri, J. Vadivelu, F. Yusof, W.J. Basirun, K. Wasa, J. Mech. Behav. Biomed. Mater. **69**, 1 (2017)
[124] F. Yildiz, A.F. Yetim, A. Alsaran, I. Efeoglu, Wear **267**, 695 (2009)
[125] J. Kusiński, S. Kac, K. Kowalski, S. Dosta, E.P. Georgiou, J. Garcia-Forgas, P. Matteazzi, Arch. Metall. Mater. **63**, 867 (2018)
[126] D. Liu, H. Xie, Z. Ma, W. Zhang, H. Zhao, L. Ren, J. Mater. Res. Technol. **19**, 2907 (2022)
[127] E.F. Morgan, G.U. Unnikrisnan, A.I. Hussein, Annu. Rev. Biomed. Eng. **20**, 119 (2018)
[128] P.F. Manicone, P. Rossi Iommetti, L. Raffaelli, J. Dent. **35**, 819 (2007)
[129] M.M. Soliman, M.E.H. Chowdhury, M.T. Islam, F. Musharavati, M. Nabil, M. Hafizh, A. Khandakar, S. Mahmud, E.Z. Nezhad, M.N.I. Shuzan, F.F. Abir, Polymers **14**, 4308 (2022)
[130] N. Shahemi, S. Liza, A.A. Abbas, A.M. Merican, J. Mech. Behav. Biomed. Mater. **87**, 1 (2018)
[131] S. Affatato, A. Ruggiero, J.S. de Mattia, P. Taddei, Compos. B Eng. **92**, 290 (2016)
[132] B. Gervais, A. Vadean, M. Raison, M. Brochu, Case Stud. Eng. Fail Anal. **5–6**, 30 (2016)
[133] M. Paliwal, D. Gordon Allan, P. Filip, Eng. Fail. Anal. **17**, 1230 (2010)
[134] E.A. Magnissalis, S. Zinelis, T. Karachalios, G. Hartofilakidis, J. Biomed. Mater. Res. B Appl. Biomater. **66B**, 299 (2003)
[135] B.F. Shahgaldi, J. Compson, Injury **31**, 85 (2000)
[136] K.K. Das, S.N. Das, S.A. Dhundasi, Indian J. Med. Res. **128**, 412 (2008)
[137] L. Leyssens, B. Vinck, C. Van Der Straeten, F. Wuyts, L. Maes, Toxicology **387**, 43 (2017)
[138] C. Exley, Morphologie **100**, 51 (2016)
[139] K. Shekhawat, S. Chatterjee, B. Joshi, Int. J. Adv. Res. **3**, 167 (2015)
[140] D. Rehder, Met. Ions Life Sci. **13**, 139 (2013)
[141] L. Yuan, S. Ding, C. Wen, Bioact. Mater. **4**, 56 (2019)
[142] Z. Tang, Y. Xie, F. Yang, Y. Huang, C. Wang, K. Dai, X. Zheng, X. Zhang, PLoS ONE **8**, 0066263 (2013)
[143] A. Hindy, F. Farahmand, F. Sadat Tabatabaei, Lasers Med. Sci. **32**, 1197 (2017)
[144] C.S. Adams, V. Antoci, G. Harrison, P. Patal, T.A. Freeman, I.M. Shapiro, J. Parvizi, N.J. Hickok, S. Radin, P. Ducheyne, J. Ortho. Res. **27**, 701 (2009)
[145] Y. Yao, S. Liu, M.V. Swain, X. Zhang, K. Zhao, Y. Jian, Mater. Sci. Eng. C **94**, 200 (2019)
[146] N.V. Abhijith, D. Kumar, D. Kalyansundaram, J. Therm. Spray Technol. **31**, 1032 (2022)
[147] F. Wang, C. Li, S. Zhang, H. Liu, Surf. Coat. Technol. **382**, 125161 (2020)
[148] S. Stübinger, A. Drechsler, A. Bürki, K. Klein, P. Kronen, B. Von Rechenberg, J. Biomed. Mater. Res. B Appl. Biomater. **104**, 1182 (2016)
[149] J.K. Xiao, H. Tan, Y.Q. Wu, J. Chen, C. Zhang, Surf. Coat. Technol. **385**, 125430 (2020)
[150] N. Tüten, D. Canadinc, A. Motallebzadeh, B. Bal, Intermetallics **105**, 99 (2019)
[151] A. Meghwal, S. Singh, A. Anupam, H.J. King, C. Schulz, C. Hall, P. Munroe, C.C. Berndt, A.S.M. Ang, J. Alloys Compd. **912**, 165000 (2022)
[152] J.E. Ahn, Y.K. Kim, S.H. Yoon, K.A. Lee, Met. Mater. Int. **27**, 2406 (2021)
[153] N.S. Peighambardoust, A.A. Alamdari, U. Unal, A. Motallebzadeh, J. Alloys Compd. **883**, 160786 (2021)
[154] A.K. Lynn, D.L. DuQuesnay, Biomaterials **23**, 1937 (2002)
[155] N. Mirhosseini, P.L. Crouse, M.J.J. Schmidth, L. Li, D. Garrod, Appl. Surf. Sci. **253**, 7738 (2007)
[156] S. Mukherjee, S. Dhara, P. Saha, Int. J. Adv. Manuf. Technol. **76**, 5 (2015)
[157] J. Mesquita-Guimarães, R. Detsch, A.C. Souza, B. Henriques, F.S. Silva, A.R. Boccaccini, O. Carvalho, Mater. Sci. Eng. C **109**, 110492 (2020)
[158] A. Purnama, V. Furlan, D. Dessi, A.G. Demir, R. Tolouei, C. Paternoster, L. Levesque, B. Previtali, D. Mantovani, A. Gökhan Demir, Surf. Eng. **36**, 1240 (2020)
[159] S.A. Wilks, H. Michels, C.W. Keevil, Int. J. Food Microbiol. **105**, 445 (2005)
[160] S.A. Wilks, H.T. Michels, C.W. Keevil, Int. J. Food Microbiol. **111**, 93 (2006)
[161] J.O. Noyce, H. Michels, C.W. Keevil, J. Hosp. Infect. **63**, 289 (2006)
[162] J.O. Noyce, H. Michels, C.W. Keevil, Appl. Environ. Microbiol. **73**, 2748 (2007)
[163] A. Kumar, H. Singh, R. Kant, N. Rasool, J. Therm. Spray Technol. **30**, 2099 (2021)

[164] J. Tang, Z. Zhao, X. Cui, J. Wang, T. Xiong, Sci. China Technol. Sci. **63**, 731 (2020)
[165] Z. Zhao, F. Meng, J. Tang, H. Liu, H. Liu, L. Yang, J. Wang, T. Xiong, Mater. Lett. **245**, 211 (2019)
[166] B. Al-Mangour, R. Mongrain, E. Irissou, S. Yue, Surf. Coat. Technol. **216**, 297 (2013)
[167] C. Wang, Z. Li, H. Zhao, G. Zhang, T. Ren, Y. Zhang, Tribol. Int. **152**, 106475 (2020)